

广东河台金矿区印支期花岗岩与混合岩成因联系及大地构造意义*

焦骞骞¹ 贺昌坤¹ 董有浦¹ 许德如^{2,3**} 陈根文³ 陈诚¹ 师爽¹ 高亦文⁴

JIAO QianQian¹, HE ChangKun¹, DONG YouPu¹, XU DeRu^{2,3**}, CHEN GenWen³, CHEN Cheng¹, SHI Shuang¹ and GAO YiWen⁴

1. 昆明理工大学国土资源工程学院, 昆明 650093

2. 东华理工大学核资源与环境国家重点实验室, 南昌 330013

3. 中国科学院广州地球化学研究所, 中国科学院矿物学与成矿学重点实验室, 广州 510640

4. 广东省地质局第五地质大队, 肇庆 526600

1. Faculty of Land Resource Engineering, Kunming University of Science and Technology, Kunming 650093, China

2. State Key Laboratory for Nuclear Resources and Environment, East China University of Technology, Nanchang 330013, China

3. CAS Key Laboratory of Mineralogy and Metallogeny, Guangzhou Institute of Geochemistry, Chinese Academy of Sciences, Guangzhou 510640, China

4. The 5th Brigade of Guangdong Geological Bureau, Zhaoqing 526600, China

2018-12-25 收稿, 2020-01-02 改回.

Jiao QQ, He CK, Dong YP, Xu DR, Chen GW, Chen C, Shi S and Gao YW. 2020. The petrogenetic links of Indosinian granitoid and migmatite in the Hetai goldfield, Guangdong Province of South China and the tectonic implication. *Acta Petrologica Sinica*, 36(3):893–912, doi:10.18654/1000-0569/2020.03.15

Abstract The Hetai goldfield of Guangdong Province is located at the Yunkai area, the junction of Guangdong and Guangxi provinces of South China. The goldfield is a favorable place for the study of the petrogenesis links of migmatite and granitoid, because of the coexistence of Indosinian plutons, migmatites and ductile shear zones. A new LA-ICP-MS U-Pb zircon age of the Yunlougang granodiorite pluton and Yunkai migmatite is 253 ± 1.6 Ma and 240.3 ± 5.1 Ma, indicating the time of magmatism is ca. 10 Myr earlier than the migmatization within analytical errors. The Yunlougang pluton and Yunkai migmatite share some geochemical characteristics, for example, they are both peraluminous, both have high K₂O, Rb, Pb, LREE contents, Fe₂O₃/MgO and (⁸⁷Sr/⁸⁶Sr)_i ratios, negative $\epsilon_{Nd}(t)$ values, low 10,000Ga/Al ratios, the depletion of Ba, Nb, Sr, P and Ti, and the negative correlation between SiO₂ and TiO₂, Fe₂O₃^T, CaO, Nb, suggesting they are likely from the crust remelting. Moreover, the biotite in them are all re-equilibrated primary biotite, indicating they were likely modified at almost the same *P-T* conditions after their diagenesis. However, the REE and Sr-Nd isotopes are distinction between the Yunlougang pluton and the Yunkai Group migmatite and meta-sedimentary. The Yunlougang pluton has Nd model ages (1821 ~ 1692 Ma) younger than the Yunkai Group migmatite (2264 ~ 1788 Ma) and meta-sedimentary (2170 ~ 1910 Ma), and smaller Rb/Sr ratio (1.4 ~ 1.8) than that of the migmatite (2.7 ~ 9.2), indicating the pluton is likely derived from a hybrid magma of anatexic lower crust with small juvenile externally (mantle) magma, the migmatite simply from the in-situ remelting of Yunkai Group meta-sedimentary. Therefore, the Yunlougang pluton is not congenetic with the migmatite nearby, not the final product of Yunkai Group migmatization. The age of Yunlougang pluton and Yunkai Group migmatite are likely represent the peak and terminal time of the collision between South China Block and Indochina Block.

Key words Yunlougang granodiorite; Yunkai Group Migmatite; Indosinian; Yunkai area

摘要 广东省河台金矿区位于两广交界的云开地区, 矿区内印支期花岗岩、混合岩和韧性剪切带并存, 是研究花岗岩与混合岩岩石成因关系的良好场所。通过 LA-ICP-MS 锆石 U-Pb 定年获得矿区内云楼岗花岗岩的年龄为 253 ± 1.6 Ma, 云开

* 本文受国家自然科学基金项目(41902086)、国家重点研发计划项目(2016YFC0600401)和昆明理工大学地质资源与地质工程省级一流学科建设项目(1407839305)联合资助。

第一作者简介: 焦骞骞, 男, 1986 年生, 博士, 从事构造地质学教学与科研, E-mail: 289284567@qq.com

** 通讯作者: 许德如, 男, 1966 年生, 教授, 博士生导师, 从事大陆边缘与成矿学研究, E-mail: xuderu@gig.ac.cn

群混合岩年龄为 240.3 ± 5.1 Ma, 在分析误差范围内前者形成时间比后者早了约 10 Myr。云楼岗花岗岩闪长岩与云开群混合岩具有某些类似的地球化学特征: 过铝质; 高的 K_2O 含量、 Fe_2O_3/MgO 比值以及 Rb、Pb、LREE 含量和初始 ($^{87}Sr/^{86}Sr$) (I_{Sr}) 比值; $\epsilon_{Nd}(t)$ 为负值; 具有低的 $10000Ga/Al$ 值; 亏损 Ba、Nb、Sr、P 和 Ti; SiO_2 与 TiO_2 、 $Fe_2O_3^+$ 、CaO、Nb 都具有负相关关系; 这些特征表明它们可能都是壳源的。另外, 两者中的黑云母都是再平衡的原生黑云母, 表明成岩后两种岩石又在近乎相同的温压条件下遭受了改造。然而, 云楼岗花岗岩闪长岩与云开群混合岩、变质沉积岩之间的稀土特征和 Sr-Nd 同位素又有所差异。前者 Nd 模式年龄为 1821 ~ 1692 Ma, 明显晚于后两者 (2264 ~ 1783 Ma, 2170 ~ 1910 Ma); 另外, 岩体的 Rb/Sr 比值为 1.4 ~ 1.8, 明显低于混合岩的 2.7 ~ 9.2。所以, 云楼岗花岗岩闪长岩可能来自下地壳深熔作用, 并混入有少量年轻地幔成分而形成的混合岩浆, 而云开群混合岩只是变质沉积岩的原地熔融产物。因此, 云楼岗花岗岩闪长岩体与邻近云开群混合岩不是同源的, 前者也不是后者的最终产物。云楼岗岩体和云开群混合岩的形成时间可能分别代表了华南板块和印支板块碰撞高峰期和终了期。

关键词 云楼岗花岗岩闪长岩; 云开群混合岩; 印支期; 云开地区

中图法分类号 P588.122; P597.3

两广交界(粤西-桂东南)的云开大山地区位于扬子板块与华夏板块之间的过渡地带。由于其所处的特殊大地构造位置, 因此不同学者曾先后使用云开隆起(广西壮族自治区地质矿产局, 1985; 汪劲草等, 1994)、云开地体(康云骥, 2001; Wan *et al.*, 2010)、云开褶皱带(郭福祥, 1994)、云开地块(Wang *et al.*, 2007a)、云开构造带(Wang *et al.*, 2007b)、云开造山带(Liang and Li, 2005; Li *et al.*, 2010; Feng *et al.*, 2014)等术语概括其大地构造属性。扬子板块与华夏板块自新元古代拼合形成华南板块后, 又至少先后经历了加里东期、印支期和燕山期三期构造-热事件(Wang *et al.*, 2011)。受多期构造-热事件的影响, 云开地区加里东期、印支期和燕山期花岗岩均有出露, 并且还发育大面积混合岩和多条韧性剪切带。因此, 云开地区是国内研究花岗岩与混合岩岩石成因关系的一个良好场所而受到关注(张伯有和俞鸿年, 1992; 王联魁等, 2003)。

花岗岩与混合岩之间可能的成因联系是成因岩石学研究的重要课题(Johannes *et al.*, 2003; Sepahi *et al.*, 2013; Suga *et al.*, 2016), 而岩浆的形成、分离结晶、上升、侵位, 是地壳物质及能量从深部到浅部的重要交换过程, 对研究大陆地壳演化有重要意义, 因此前人对此进行过大量研究(England and Thompson, 1986; Simpson *et al.*, 2000; Solar and Brown, 2001; Annen *et al.*, 2006; Brown, 2007; Qiu *et al.*, 2014)。混合岩多在深熔作用下产于变质程度高的地层中(Sawyer, 1998, 2001), 由于原岩在不同温-压条件下发生熔融和分离结晶的程度有所不同, 因此形成的混合岩的岩石结构构造、矿物组成及化学成分也有所差异, 总的可以分为两大类, 即变熔混合岩和全熔混合岩(Brown *et al.*, 1995; Milord *et al.*, 2001; Solar and Brown, 2001; Suga *et al.*, 2016)。变熔混合岩熔融程度较低, 整体还处于固态, 仍保留了部分熔融前的原岩结构, 长英质脉体(熔融体)与暗色基体(残留体)间呈厘米级间隔(Sawyer, 1994, 2001; Brown, 1994; Brown *et al.*, 1995)。而全熔混合岩中, 原岩熔融程度和熔体分离程度都较高, 结构几乎完全破坏, 岩石结构均一化, 矿物颗粒增大, 残留的原岩固体部分已失去凝聚力, 与熔融体一起形成高粘度的“晶粥”, 或者成为能迁移的塑性体,

其流变学特征已类似于岩浆(Sawyer, 1998; Milord *et al.*, 2001; White *et al.*, 2005; Suga *et al.*, 2016)。Milord *et al.* (2001) 根据岩石中暗色矿物(主要是黑云母)含量, 将全熔混合岩分为三类: 深色、中色和浅色全熔混合岩, 黑云母含量分别为 $>30\%$ 、 $10\% \sim 30\%$ 和 $<10\%$ 。重熔花岗岩一般是浅色的, 在成因上可能与其周围的混合岩有关, 是混合岩中熔融部分与残余部分分离后在合适的位置聚集结晶而成(Milord *et al.*, 2001; Solar and Brown, 2001), 另外可能还有一些外部岩浆及含水流体的加入, 从而增加了熔体的量(Johannes *et al.*, 2003)。然而, 在云开地区, 混合岩周边却分布着一些暗色的 S 型花岗岩岩体, 例如在河台金矿区西北部出露的印支期云楼岗岩体, 它在成因上与河台金矿区中大量的混合岩是什么关系呢? 张伯有和俞鸿年(1992)认为云开地区混合岩是由糜棱岩改造而来, 而花岗岩则是混合岩化的最终产物, 但是缺少相应的年代学及地球化学证据。王联魁等(2003)按形成方式将花岗岩分为三类, 即混合岩建造、深熔花岗岩建造和岩浆花岗岩建造, 并对云开地区花岗岩的岩石学、地球化学特征及形成条件进行了较为详细的研究, 但是并未深入讨论它们之间的成因关系。因此, 本文将以云开地区河台金矿区内云开群混合岩及云楼岗岩体为研究对象, 通过岩石学、矿物学、地球化学、地质年代学的研究, 探讨暗色的 S 型花岗岩与混合岩之间的成因关系, 从而进一步丰富岩浆岩的成因岩石学理论, 并为云开地区大地构造演化提供新的证据。

1 构造背景

华南板块由扬子板块和华夏板块构成, 其界线为江山-绍兴缝合带(图 1a), 但由于多期强烈构造事件的叠加, 该缝合带向南西延伸逐渐模糊不清, 导致两板块的南西边界有较大争议(图 1a, Yan *et al.*, 2006; Wan, 2012)。云开地区位于华夏板块的西北部边界, 区域内出露的云开群和高州杂岩过去通常被作为华夏地块的前寒武变质基底, 其上覆未变质-弱变质的奥陶系-白垩系(图 1b), 然而, 最新研究表明, 这两套地层实为同一套地层, 统称为云开群, 两者沉积时代相

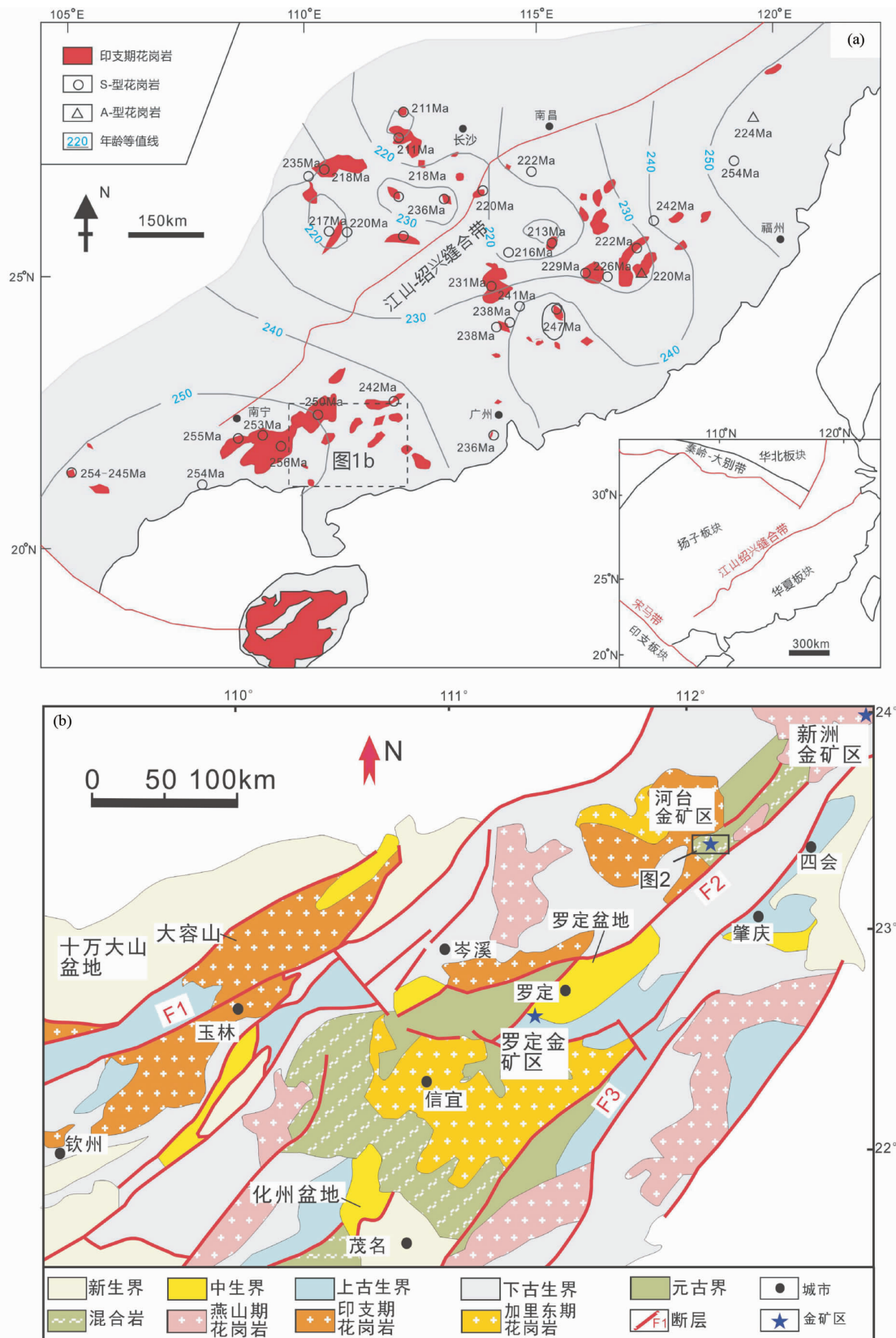


图1 华南地区大地构造及印支期花岗岩分布图(a, 据 Qiu *et al.*, 2014 修改)和云开地区地质简图(b, 据丘元禧和梁新权, 2006; 彭松柏等, 2006 修改)

Fig.1 Tectonic sketch map of South China Block and the distribution of the Indosinian granitoids (a, after Qiu *et al.*, 2014) and regional geological map of Yunkai area (b, after Qiu and Liang, 2006; Peng *et al.*, 2006)

同,为晚新元古代-早古生代,并非古元古代-早新元古代(叶真华等, 2000; 邝永光等, 2001; Wang *et al.*, 2007a; Wan *et al.*, 2010; Chen *et al.*, 2012; 周雪瑶等, 2015; 焦骞骞等, 2017)。云开群变质程度由绿片岩相到麻粒岩相,岩性为片岩、千枚岩、板岩,局部为片麻岩、角闪岩、麻粒岩、混合岩。锆石 U-Pb 定年表明,云开群经历了两期变质作用,一期集中在约 440Ma,与加里东运动有关;在印支期约 240Ma 时,云开群局部又发生了再活化,形成变质程度更高的岩石,例如,混合岩、硅线石-石榴子石-堇青石片麻岩(Wang *et al.*, 2007a, 2012; Wan *et al.*, 2010)。

云开地区有大量花岗岩侵入体,时代从加里东期到燕山期均有分布。信宜花岗岩锆石 U-Pb 年龄为 460 ~ 430Ma,其形成与加里东期造山活动有关(图 1b, 彭松柏等, 2006; Wang *et al.*, 2007a; Wan *et al.*, 2010)。云开地区出露的印支期 S 型花岗岩年龄集中在 260 ~ 245Ma,少量为 230Ma,并且主要沿断裂分布(图 1b, Chen *et al.*, 2011)。例如,在广宁-罗定动力变质带北东段,特别是河台金矿区附近(邱小平, 2004);在防城-灵山断裂带附近大容山-十万大山也有大量 S 型花岗岩(祁昌实等, 2007; Jiao *et al.*, 2015)。在燕山期侵入形成大量未变形的 I 型花岗岩沿着云开地区西南边缘分布(蔡明海等, 2002; 邱小平, 2004; Wang *et al.*, 2007a; Lin *et al.*, 2008)。区域上构造线以 NE-NNE 方向为主,可见几条近于平行的剪切带系统,例如防城-灵山断裂 F1,罗定-广宁断裂 F2,吴川-四会断裂 F3 等(图 1b)。这些区域性大断裂(韧性剪切带)主要是在印支期造山作用下经过约 248 ~ 220Ma 和 220 ~ 200Ma 两期构造活动形成的(Wang *et al.*, 2007a; 丁汝鑫等, 2015; Jiao *et al.*, 2017),并且控制着区域内矿产的分布和产出。例如,沿着罗定-广宁断裂有新洲金矿区、河台金矿区、罗定金矿区的分布,其中河台金矿区是本文的主要研究对象。

2 矿区地质及岩石学特征

河台矿区及外围出露的地层主要有云开群、奥陶系、志留系(图 2)。云开群分布在矿区北部,为一套整体无序的变质岩组成,岩性以变粒岩、片麻岩、混合岩为主,局部遭受强烈韧性剪切作用形成糜棱岩系列岩石,河台金矿的矿体就产于这些糜棱岩带(ML9、ML11、ML12、ML13、ML18)中。奥陶系与志留系分布在矿区南部,以薄层浅变质砂岩、粉砂岩、及薄层板岩为主,通过 F1 断裂与云开群地层接触。矿区西部出露印支期云楼岗岩体;矿区东北部为燕山期的伍村巨斑状黑云母花岗岩,单颗粒锆石 U-Pb 年龄 $153.6 \pm 2.1\text{Ma}$ (翟伟等, 2005)。

2.1 云楼岗岩体岩石学特征

云楼岗岩体出露面积大于 100km^2 ,岩性主要为中粗粒黑云母二长花岗岩、黑云母斜长花岗岩,具花岗结构、块状构

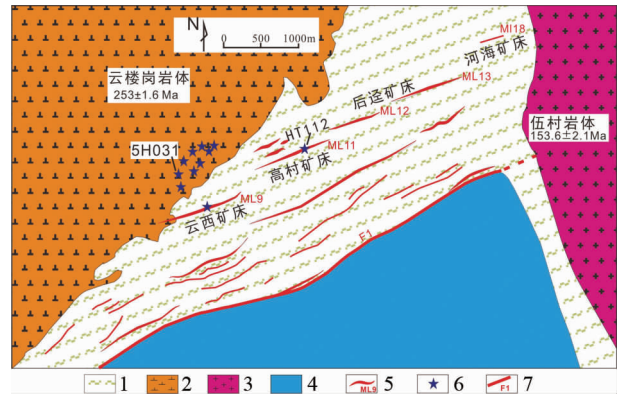


图 2 河台矿区地质图(据陈骏和王鹤年, 1993 修改)

1-云开群混合岩;2-云楼岗花岗岩;3-伍村斑状黑云母花岗岩;4-奥陶系与志留系薄层浅变质砂岩、粉砂岩、及薄层板岩;5-糜棱岩带及编号;6-采样位置;7-宝鸭塘-坑尾断裂

Fig. 2 Geological sketch map of Hetai gold deposit (modified after Chen and Wang, 1993)

1-Yunkai Group migmatite; 2-Yunlougang granodiorite; 3-Wucun porphyritic biotite granite; 4-Ordovician and Silurian flaggy weak metamorphic sandstone-siltite and flaggy killas; 5-mylonite zone and serial number; 6-sampling location; 7-Baoyatang-Kengwei fault

造(图 3a, b),局部受剪切形成糜棱岩化花岗岩。岩石主要由长石(55%)、石英(20%)、黑云母(20%)和白云母(5%)组成(图 3c, d)。其中黑云母呈自形-半自形,与长石和石英近于同时形成,在其边部分布有较小的白云母。前人利用全岩 Rb-Sr 法、单颗粒锆石全熔法等获得年龄为 242 ~ 209Ma(崔遥, 1989; 叶伯丹, 1989)。由于这些方法精度不高或者缺少锆石的形态结构特征,因此可靠性难以评价。本次研究将利用 LA-ICP-MS 锆石 U-Pb 法对其进行精确测年。

2.2 云开群混合岩岩石学特征

河台矿区内分布着大面积的云开群混合岩,这些混合岩大多属于全熔混合岩,混合岩化之前的岩石结构已完全破坏,岩石中矿物颗粒均一化、粗粒化。从颜色及矿物成分看,属于中色、浅色的全熔混合岩,主要由长石(55%)、石英(25%)、黑云母(10%)、白云母(5%)和绢云母集合体(5%)组成(图 3e, f)。由于距离剪切带较近,受其影响,长石边缘有明显细粒化现象,绢云母分布于长石裂隙中,表明其晚于长石,可能与后期热液活动有关。

3 样品采集及实验方法

9 个花岗岩样品采自河台矿区云楼岗岩体东部,并且靠近云开群混合岩的位置(图 2)。7 个混合岩样品采自高村金矿 -140m 中段和云西金矿 +10m 中段(图 2)。野外所采集的花岗岩样品表面风化较强(图 3a, b),首先对其进行实验前处理,将表面风化部分去除掉,以免影响实验结果。

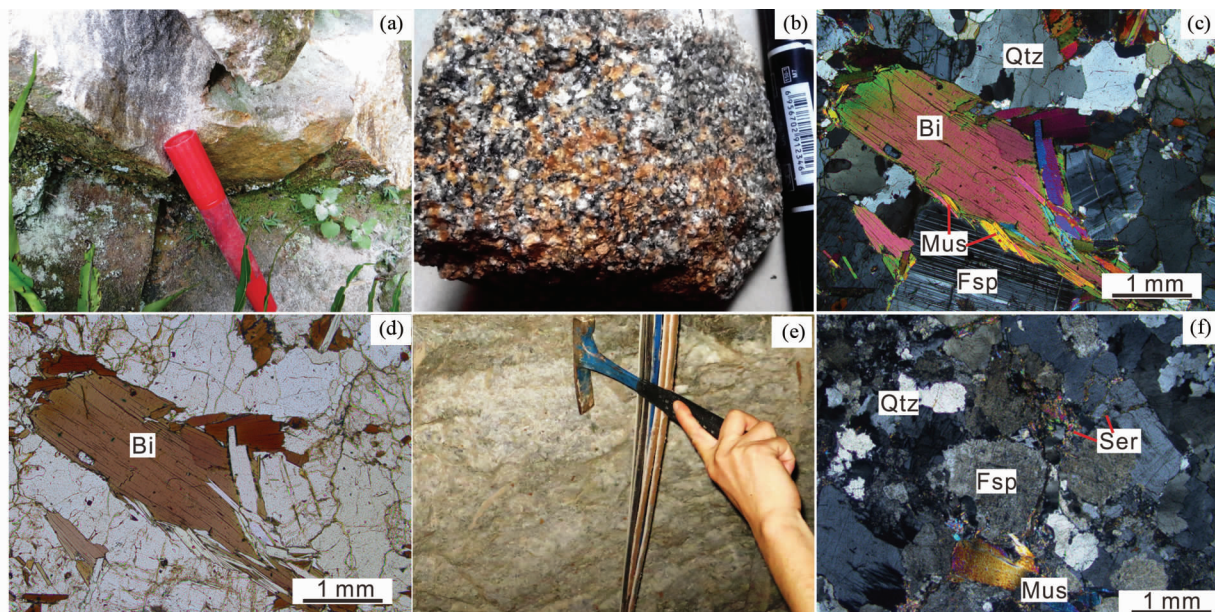


图3 岩石样品野外及镜下照片

(a) 云楼岗岩体野外露头, 记号笔长约 14cm; (b) 云楼岗花岗岩闪长岩手标本; (c, d) 云楼岗岩体显微照片, 黑云母为自形-半自形, 边部有细小的白云母颗粒, c 为正交偏光, d 为单偏光; (e) 云开群混合岩井下露头; (f) 云开群混合岩显微照片 (正交偏光), 长石颗粒边部有明显的细粒化现象, 绢云母产于长石裂隙中, 形成时间相对较晚。Qtz-石英; Fsp-长石; Bi-黑云母; Mus-白云母; Ser-绢云母

Fig. 3 Field photographs and microphotographs of Yunlougang granodiorite and Yunkai Group migmatite

(a) field outcrop of Yunlougang pluton, length of the marking pen is 14cm; (b) hand specimen of the Yunlougang granodiorite; (c, d) microphotographs of the Yunlougang granodiorite, euhedral to subhedral biotite with small muscovite along its margin; (e) outcrop of diatexite migmatite from the Gaocun gold deposit at -140m elevation; (f) microphotographs of the diatexite migmatite. Margin of feldspar has notable fine grained, relatively late sericite aggregation in fracture of feldspar. Photomicrograph (c and f) from crossed nicols; and (d) from plane nicols. Qtz-quartz; Fsp-feldspar; Bi-biotite; Mus-muscovite; Ser-sericite

3.1 LA-ICP-MS 锆石 U-Pb 定年

锆石分选在河北省诚信服务有限公司完成, 采用常规方法将样品粉碎至 80 目以上, 并采用电磁选方法进行分选。在双目镜下挑选出晶形和透明度较好, 无裂纹, 粒径足够大的锆石颗粒作为测试对象。锆石制靶和阴极发光 (CL) 图像在重庆宇劲科技有限公司完成。锆石年龄测试在中国科学院广州地球化学研究所矿物学与成矿学中国科学院重点实验室完成, 使用仪器为 LA-ICP-MS, 仪器型号为 Resolution M50 Agilent 7500a, 厂家 Resonetics Agilent, 光斑为 29 μ m。采用标准锆石 Plesovice ($^{206}\text{Pb}/^{238}\text{U}$ 加权平均年龄为 337.13 \pm 0.37Ma (Sláma *et al.*, 2008)) 和 Temora ($^{206}\text{Pb}/^{238}\text{U}$ 加权平均年龄为 416.6 \pm 1.0Ma (Black *et al.*, 2003)) 作为外标, 元素含量采用 NIST SRM610 作为外标, ^{29}Si 作为内标元素 (锆石中 SiO_2 含量为 32.8%) (袁洪林等, 2003), 分析方法参考 Yuan *et al.* (2004) 方法; 普通铅校正采用 Andersen (2002) 推荐的方法; 锆石的同位素比值及微量稀土元素含量计算采用 ICPMSDATECAL 程序 (Liu *et al.*, 2008, 2010), 年龄计算及谐和图的绘制采用 Isoplot 2006 (Ludwig, 2003)。

3.2 全岩地球化学和 Sr-Nd 同位素测试

将新鲜的花岗岩和混合岩样品磨碎到 200 目, 以备主微

量和 Sr-Nd 同位素测试。测试工作在中国科学院广州地球化学研究所同位素地球化学国家重点实验室完成。

主量元素利用 Rigaku 100e XRF 进行测试, 分析结果的误差 (相对标准偏差值) 小于 3% (H_2O^+ 除外)。样品粉末加入 $\text{Li}_2\text{B}_4\text{O}_7$ (1:8), 在 V8C 自动熔融机 (AnalyMate, 中国) 熔融机上加热至 1150 ~ 1200 $^\circ\text{C}$, 制成均一的玻璃片, 然后进行 X 射线荧光 (XRF) 分析。

微量元素分析在 Agilent 7700X 型电感耦合等离子体质谱仪 (ICP-MS) 上进行分析, 稀土元素和 Y 分析误差小于 4%, 其它微量元素在 3% ~ 7% 之间。将约 40mg 样品粉末放入 Teflon 杯中并加入 $\text{HF} + \text{HNO}_3$, 100 $^\circ\text{C}$ 加热 7 天溶解。之后烘干并加入 3% 的 HNO_3 , 进行测试。利用 Rh 作为内标进行校正 (Liu *et al.*, 1996)。

分离纯化后的 Sr 和 Nd 溶液在 Micromass Isoprobe 型多接收器等离子质谱仪 (MC ICP-MS) 上进行 $^{87}\text{Sr}/^{86}\text{Sr}$ Sr 和 $^{142}\text{Nd}/^{144}\text{Nd}$ 比值测定, 详细的测试方法见 Li *et al.* (2006)。测试过程中的质量分馏效应分别采用 $^{86}\text{Sr}/^{88}\text{Sr} = 0.1194$ 和 $^{146}\text{Nd}/^{144}\text{Nd} = 0.7219$ 进行校正。Shin Etsu JNdi-1 标准的 $^{143}\text{Nd}/^{144}\text{Nd}$ 和 $^{87}\text{Sr}/^{86}\text{Sr}$ 测定值为分别 0.512115 (2σ) 和 0.710260 (2σ)。

表1 云楼岗花岗闪长岩和云开群混合岩锆石 LA-ICP-MS U-Pb 年龄

Table 1 Zircon LA-ICP-MS U-Pb ages of the Yunlougang granodiorite and the Yunkai Group migmatite

| 测点号 | Th U | | Th/U | 同位素比值 | | | | | 同位素年龄(Ma) | | | | | 协和度 (%) | | |
|-------------------|----------------------|------|------|---|------------|--|------------|--|------------|---|------------|--|------------|---------|--|------------|
| | ($\times 10^{-6}$) | | | $\frac{^{207}\text{Pb}}{^{206}\text{Pb}}$ | 1 σ | $\frac{^{207}\text{Pb}}{^{235}\text{U}}$ | 1 σ | $\frac{^{206}\text{Pb}}{^{238}\text{U}}$ | 1 σ | $\frac{^{207}\text{Pb}}{^{206}\text{Pb}}$ | 1 σ | $\frac{^{207}\text{Pb}}{^{235}\text{U}}$ | 1 σ | | $\frac{^{206}\text{Pb}}{^{238}\text{U}}$ | 1 σ |
| 样品 5H031 云楼岗花岗闪长岩 | | | | | | | | | | | | | | | | |
| -08 | 19.0 | 488 | 0.04 | 0.0514 | 0.00 | 0.2872 | 0.02 | 0.0402 | 0.00 | 387 | 109 | 274 | 14 | 258 | 5 | 94 |
| -12 | 55.0 | 692 | 0.08 | 0.0501 | 0.00 | 0.2694 | 0.01 | 0.0393 | 0.00 | 211 | 97 | 242 | 10 | 248 | 3 | 97 |
| -13 | 43.4 | 546 | 0.08 | 0.0506 | 0.00 | 0.2778 | 0.01 | 0.0402 | 0.00 | 76.0 | 115 | 229 | 12 | 249 | 4 | 91 |
| -14 | 44.8 | 431 | 0.10 | 0.0508 | 0.00 | 0.2786 | 0.01 | 0.0401 | 0.00 | 176 | 99 | 244 | 10 | 249 | 3 | 97 |
| -15 | 4.55 | 294 | 0.02 | 0.0497 | 0.00 | 0.2716 | 0.01 | 0.0399 | 0.00 | 309 | 111 | 256 | 11 | 250 | 3 | 97 |
| -16 | 10.8 | 193 | 0.06 | 0.0519 | 0.00 | 0.2840 | 0.02 | 0.0400 | 0.00 | 280 | 160 | 254 | 13 | 250 | 4 | 98 |
| -17 | 127 | 399 | 0.32 | 0.0499 | 0.00 | 0.2735 | 0.01 | 0.0399 | 0.00 | 235 | 93 | 250 | 9 | 251 | 4 | 99 |
| -18 | 48.2 | 122 | 0.39 | 0.0533 | 0.00 | 0.2976 | 0.01 | 0.0406 | 0.00 | 211 | 144 | 242 | 13 | 252 | 4 | 96 |
| -19 | 59.5 | 116 | 0.52 | 0.0544 | 0.00 | 0.3092 | 0.02 | 0.0408 | 0.00 | 187 | 98 | 245 | 10 | 252 | 3 | 97 |
| -20 | 38.1 | 92.6 | 0.41 | 0.0505 | 0.00 | 0.2735 | 0.01 | 0.0400 | 0.00 | 189 | 119 | 244 | 11 | 252 | 4 | 96 |
| -22 | 51.6 | 193 | 0.27 | 0.0526 | 0.00 | 0.2866 | 0.01 | 0.0396 | 0.00 | 283 | 158 | 254 | 13 | 253 | 3 | 99 |
| -24 | 66.6 | 605 | 0.11 | 0.0509 | 0.00 | 0.2798 | 0.01 | 0.0398 | 0.00 | 217 | 129 | 246 | 11 | 253 | 4 | 97 |
| -25 | 13.2 | 360 | 0.04 | 0.0496 | 0.00 | 0.2713 | 0.01 | 0.0394 | 0.00 | 217 | 94 | 251 | 9 | 253 | 4 | 99 |
| -26 | 86.2 | 245 | 0.35 | 0.0518 | 0.00 | 0.2845 | 0.02 | 0.0396 | 0.00 | 280 | 94 | 257 | 10 | 253 | 3 | 98 |
| -27 | 21.6 | 573 | 0.04 | 0.0519 | 0.00 | 0.2883 | 0.01 | 0.0401 | 0.00 | 232 | 96 | 250 | 10 | 254 | 4 | 98 |
| -28 | 26.8 | 111 | 0.24 | 0.0484 | 0.00 | 0.2699 | 0.01 | 0.0403 | 0.00 | 257 | 107 | 256 | 12 | 254 | 4 | 99 |
| -29 | 23.5 | 468 | 0.05 | 0.0499 | 0.00 | 0.2799 | 0.01 | 0.0403 | 0.00 | 233 | 94 | 249 | 10 | 254 | 3 | 97 |
| -30 | 53.6 | 502 | 0.11 | 0.0505 | 0.00 | 0.2806 | 0.01 | 0.0400 | 0.00 | 117 | 86 | 243 | 11 | 255 | 5 | 95 |
| -31 | 38.4 | 101 | 0.38 | 0.0502 | 0.00 | 0.2695 | 0.02 | 0.0399 | 0.00 | 191 | 85 | 251 | 8 | 255 | 3 | 98 |
| -32 | 63.2 | 201 | 0.31 | 0.0475 | 0.00 | 0.2526 | 0.01 | 0.0394 | 0.00 | 343 | 104 | 265 | 12 | 257 | 4 | 96 |
| 样品 HT112 云开群混合岩 | | | | | | | | | | | | | | | | |
| -10 | 368 | 795 | 0.46 | 0.0524 | 0.00 | 0.2787 | 0.01 | 0.0387 | 0.00 | 302 | 62 | 250 | 6 | 245 | 4 | 98 |
| -12 | 194 | 838 | 0.23 | 0.0512 | 0.00 | 0.2585 | 0.01 | 0.0366 | 0.00 | 256 | 47 | 233 | 5 | 232 | 3 | 99 |
| -13 | 107 | 200 | 0.54 | 0.0525 | 0.00 | 0.3254 | 0.01 | 0.0453 | 0.00 | 306 | 81 | 286 | 10 | 285 | 8 | 99 |
| -14 | 425 | 296 | 1.44 | 0.0555 | 0.00 | 0.2671 | 0.01 | 0.0350 | 0.00 | 432 | 63 | 240 | 6 | 222 | 4 | 92 |
| -16 | 191 | 193 | 0.99 | 0.0499 | 0.00 | 0.2600 | 0.01 | 0.0383 | 0.00 | 191 | 112 | 235 | 8 | 242 | 5 | 96 |
| -18 | 200 | 258 | 0.78 | 0.0527 | 0.00 | 0.3132 | 0.02 | 0.0433 | 0.00 | 317 | 64 | 277 | 12 | 273 | 10 | 98 |
| -22 | 5.30 | 811 | 0.01 | 0.0497 | 0.00 | 0.2678 | 0.01 | 0.0391 | 0.00 | 189 | 54 | 241 | 5 | 247 | 3 | 97 |
| -23 | 205 | 269 | 0.76 | 0.0522 | 0.00 | 0.2613 | 0.01 | 0.0364 | 0.00 | 295 | 63 | 236 | 6 | 231 | 3 | 97 |
| -25 | 102 | 1758 | 0.06 | 0.0496 | 0.00 | 0.2854 | 0.01 | 0.0417 | 0.00 | 176 | 37 | 255 | 6 | 263 | 5 | 96 |
| -27 | 101 | 268 | 0.38 | 0.0516 | 0.00 | 0.2777 | 0.01 | 0.0390 | 0.00 | 333 | 61 | 249 | 7 | 247 | 5 | 99 |
| -29 | 99 | 121 | 0.82 | 0.0527 | 0.00 | 0.2826 | 0.01 | 0.0390 | 0.00 | 322 | 85 | 253 | 10 | 247 | 6 | 97 |
| -3 | 180 | 389 | 0.46 | 0.0523 | 0.00 | 0.3362 | 0.01 | 0.0467 | 0.00 | 298 | 68 | 294 | 10 | 294 | 8 | 99 |
| -36 | 37.2 | 1301 | 0.03 | 0.0564 | 0.00 | 0.3821 | 0.01 | 0.0491 | 0.00 | 478 | 38 | 329 | 8 | 309 | 7 | 93 |
| -37 | 369 | 349 | 1.06 | 0.0536 | 0.00 | 0.2825 | 0.01 | 0.0383 | 0.00 | 367 | 52 | 253 | 6 | 242 | 4 | 95 |
| -38 | 733 | 455 | 1.61 | 0.0527 | 0.00 | 0.2744 | 0.01 | 0.0378 | 0.00 | 317 | 52 | 246 | 6 | 239 | 4 | 97 |
| -8 | 53.0 | 379 | 0.14 | 0.0571 | 0.00 | 0.4376 | 0.01 | 0.0552 | 0.00 | 494 | 52 | 369 | 11 | 347 | 7 | 93 |
| -9 | 553 | 600 | 0.92 | 0.0513 | 0.00 | 0.2767 | 0.01 | 0.0392 | 0.00 | 254 | 46 | 248 | 5 | 248 | 4 | 99 |

差不超过3%。黑云母结构式以22个O离子数为标准进行计算, Fe^{2+} 和 Fe^{3+} 利用林文蔚和彭丽君(1994)提供的方法进行估算。

3.3 黑云母化学成分分析

对薄片进行详细观察后,选择5个具有代表性的样品薄片进行电子探针(EPMA)分析。电子探针分析在中国科学院广州地球化学研究所矿物学与成矿学中国科学院重点实验室电子探针(EMPA)实验室完成,所用仪器为日本电子JOEL公司生产的JXA-823V型电子探针,实验中加速电压为15kV,束流为 2.0×10^{-8} ,束斑大小为 $5\mu\text{m}$,矿物定量分析误

4 实验结果

4.1 地质年代学

云楼岗岩体(样品5H031)中的锆石晶形良好,多为自形

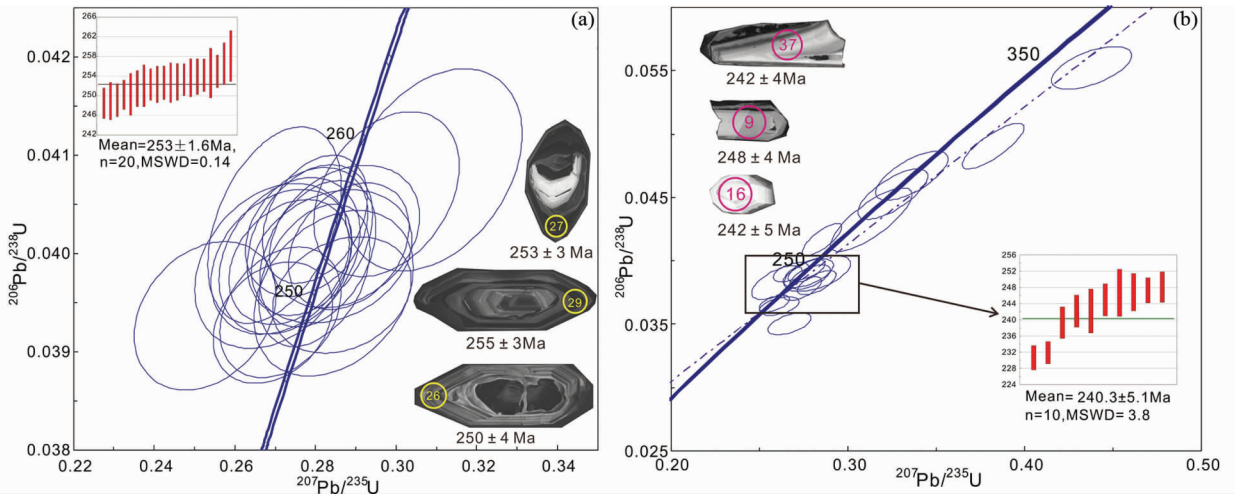


图4 云楼岗花岗闪长岩(a)和云开群混合岩(b)LA-ICP-MS 锆石 U-Pb 年龄协和图、代表性的锆石颗粒特征及年龄光斑半径为29 μm ,光斑号及年龄与表1所列一致

Fig. 4 LA-ICP-MS zircon U-Pb concordia diagrams and representative zircon grains on analyzed spots with LA-ICP-MS $^{206}\text{Pb}/^{238}\text{U}$ ages for the Yunlougang granodiorite (a) and the Yunkai Group migmatite (b)

The spots are 29 μm , identification numbers and ages as in table 1

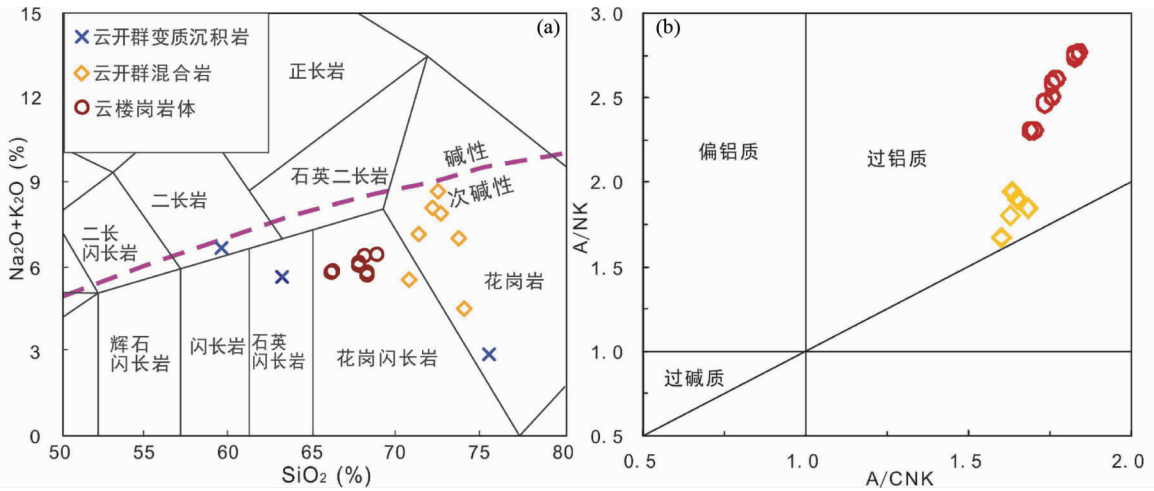


图5 岩石地球化学分类 TAS 图解 (a, 底图据 Miyashiro, 1978; Middlemost, 1994) 和 A/NK-A/CNK 图解 (b, 底图据 Chappell and White, 1992; Chappell, 1999)

烧失量不计,所有的主量元素按照全岩 100% 进行校正。图 6 图例同此图

Fig. 5 TAS Classification diagram (a, base map after Miyashiro, 1978; Middlemost, 1994) and A/NK vs. A/CNK plot (b, base map after Chappell and White, 1992; Chappell, 1999) of the granitoids

All of the major element data have been recalculated to 100% on a LOI-free basis. The meanings of graphic symbols in Fig. 6 are identical to this figure

晶,长柱状,长 100 ~ 200 μm ,长宽比 1 : 3 ~ 1 : 4。CL 图像上,锆石颗粒颜色较暗,不透明,具有典型的核-幔结构(图 4a)。锆石继承核形态多样,而锆石幔部具有明显的震荡环带,Th/U 比为 0.02 ~ 0.52,具典型的深熔岩浆锆石的特点。锆石幔部 20 个点的 $^{206}\text{Pb}/^{238}\text{U}$ 年龄为 258 ~ 248Ma(表 1、图 4a),加权平均年龄为 253 \pm 1.6Ma (MSWD = 0.14)。

云开群混合岩(样品 HT112)中的锆石形态多样,自形-他形,大多为不规则状,锆石颗粒相对较小,长 80 ~ 150 μm ,

长宽比 1 : 2 ~ 1 : 3。在 CL 图像上锆石发光性也有差别,多数发暗光,少数晶形较好的发亮光,且具有震荡环带(图 4b)。选择 17 颗形态不同的锆石中进行 U-Pb 定年,获得的 $^{206}\text{Pb}/^{238}\text{U}$ 年龄值较分散,分布在 347 ~ 222Ma(表 1、图 4b),但是其中有 10 个年龄集中在 248 ~ 231Ma,加权平均年龄为 240.3 \pm 5.1Ma (MSWD = 3.8)。另外有 6 颗锆石年龄较老且分散,在 347 ~ 263Ma,可能是由于原岩在熔融过程中,锆石没有完全被改造而继承有原岩的年龄信息,因而偏大。

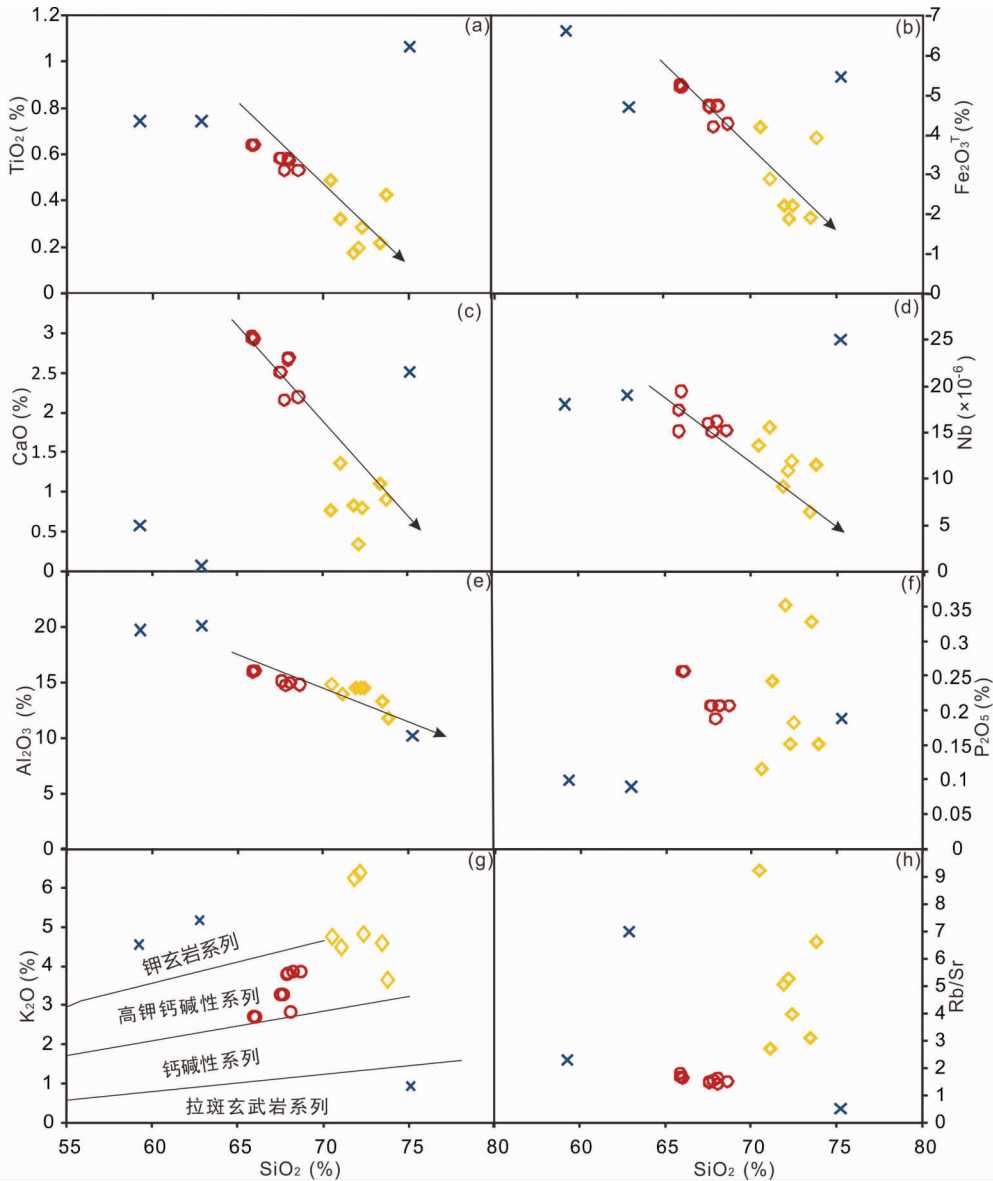


图6 哈克图解(g,底图据 Roberts and Clemens, 1993)

Fig.6 Harker diagrams comparing the composition (g, base map after Roberts and Clemens, 1993)

4.2 全岩主微量

表2为云楼岗岩体的10个样品和云开群混合岩的6个样品的主微量元素分析测试结果。

云楼岗岩体在硅-碱系列图解上属于花岗闪长岩系列(图5a),其 A/CNK ($Al_2O_3/(Na_2O + K_2O + CaO)$)值为1.17~1.21 > 1.1,为强过铝质系列(图5b)。随着 SiO_2 含量的增加, TiO_2 、 $Fe_2O_3^T$ 、 CaO 、 Al_2O_3 和Nb逐渐降低(图6a-e),而 P_2O_5 、 K_2O 和Rb/Sr没有规律性的变化(图6f-h)。岩体的 SiO_2 含量较低,为65.94%~68.68%,而 Al_2O_3 (14.70%~16.05%)、 $Fe_2O_3^T$ (4.15%~5.21%)和 Na_2O (2.56%~3.06%)含量相对较高。另外,岩体属于高K钙碱性系列(图

6g),具有低的Rb/Sr比值,为1.4~1.8(平均1.6,图6h)。在微量元素蛛网图上,云楼岗岩体强烈亏损Ba、Nb、Sr、P和Ti(图7a)。岩体 ΣREE 含量为 $109.5 \times 10^{-6} \sim 143.8 \times 10^{-6}$,富集轻稀土元素LREE($(La/Sm)_N = 3.68 \sim 4.01$),亏损重稀土元素HREE($(Ga/Yb)_N = 4.12 \sim 4.70$)。在稀土元素配分图上呈现右倾的特征(图7b), $(La/Yb)_N$ 值为20.29~23.93,平均22.80;还具有明显的Eu负异常, δEu 为0.21~0.26,表明岩浆演化中,在分离结晶作用过程中斜长石有明显的晶出。

云开群混合岩的 SiO_2 (70.57%~73.86%) 和 K_2O (3.66%~6.41%)含量,以及Rb/Sr比值(2.7~9.2)都相对较高,而 TiO_2 (0.17%~0.49%)、 $Fe_2O_3^T$ (1.82%~4.14%)和 CaO (0.34%~1.35%)含量则相对较低, Al_2O_3 含量为

表 2 云楼岗岩体和云开群混合及变质沉积岩主量 (wt%) 和微量 ($\times 10^{-6}$) 元素含量

Table 2 Major (wt%) and trace ($\times 10^{-6}$) element contents of the Yunlonggang pluton, the Yunkai Group migmatite and metasedimentary

| 样品号 | 5H171 | 5H172 | 5H173 | 5H174 | 5H175 | 5H176 | 5H031 | 5H032 | 5H033 | HT112 | HT51 | HT52 | HT54 | HT57 | HT60 | HT80 | G0103-1 | G0104-1 | G0105-1 | |
|--|-------|-------|-------|-------|-------|-------|-------|-------|-------|--------|--------|-------|-------|-------|-------|--------|---------|---------|---------|--|
| | 云楼岗岩体 | | | | | | | | | | 云开群混合岩 | | | | | | | | | |
| 岩性 | | | | | | | | | | | | | | | | | | | | |
| SiO ₂ | 68.1 | 68.68 | 67.62 | 67.63 | 67.88 | 68.11 | 65.94 | 65.94 | 66.06 | 73.50 | 72.25 | 72.46 | 73.86 | 71.16 | 71.95 | 70.57 | 62.98 | 59.35 | 75.28 | |
| Al ₂ O ₃ | 14.94 | 14.77 | 15.1 | 15.1 | 14.7 | 14.96 | 16.05 | 15.94 | 16.04 | 13.33 | 14.47 | 14.46 | 11.81 | 13.89 | 14.53 | 14.78 | 20.07 | 19.67 | 10.16 | |
| F ₂ O ₃ ^T | 4.67 | 4.23 | 4.68 | 4.65 | 4.15 | 4.68 | 5.16 | 5.21 | 5.16 | 1.87 | 1.82 | 2.17 | 3.86 | 2.83 | 2.17 | 4.14 | 4.63 | 6.55 | 5.41 | |
| MnO | 0.11 | 0.08 | 0.1 | 0.1 | 0.08 | 0.11 | 0.12 | 0.12 | 0.12 | 0.08 | 0.07 | 0.07 | 0.11 | 0.12 | 0.09 | 0.08 | 0.03 | 0.09 | 0.18 | |
| TiO ₂ | 0.58 | 0.53 | 0.58 | 0.58 | 0.53 | 0.57 | 0.64 | 0.64 | 0.64 | 0.21 | 0.19 | 0.28 | 0.42 | 0.32 | 0.17 | 0.49 | 0.74 | 0.74 | 1.06 | |
| MgO | 1.76 | 1.65 | 1.8 | 1.81 | 1.63 | 1.77 | 1.94 | 1.93 | 1.95 | 0.58 | 0.46 | 0.51 | 1.54 | 0.90 | 0.35 | 1.56 | 0.86 | 2.81 | 1.34 | |
| CaO | 2.66 | 2.19 | 2.5 | 2.5 | 2.15 | 2.68 | 2.93 | 2.95 | 2.92 | 1.10 | 0.34 | 0.80 | 0.90 | 1.35 | 0.83 | 0.76 | 0.06 | 0.57 | 2.5 | |
| K ₂ O | 2.85 | 3.87 | 3.28 | 3.29 | 3.83 | 2.88 | 2.74 | 2.75 | 2.77 | 4.62 | 6.41 | 4.85 | 3.66 | 4.53 | 6.26 | 4.76 | 5.2 | 4.55 | 0.96 | |
| Na ₂ O | 2.86 | 2.56 | 2.75 | 2.83 | 2.56 | 2.9 | 3.04 | 3.02 | 3.06 | 2.40 | 2.26 | 3.03 | 0.87 | 2.65 | 1.84 | 0.77 | 0.46 | 2.12 | 1.92 | |
| P ₂ O ₅ | 0.21 | 0.21 | 0.21 | 0.21 | 0.19 | 0.21 | 0.26 | 0.26 | 0.26 | 0.33 | 0.15 | 0.18 | 0.15 | 0.25 | 0.36 | 0.12 | 0.09 | 0.1 | 0.19 | |
| LOI | 1.11 | 0.92 | 0.82 | 1.12 | 1.61 | 0.98 | 0.83 | 0.88 | 0.88 | 2.02 | 0.99 | 0.92 | 2.41 | 1.87 | 0.85 | 2.03 | 3.94 | 2.99 | 0.66 | |
| Total | 99.85 | 99.7 | 99.45 | 99.82 | 99.32 | 99.86 | 99.65 | 99.63 | 99.85 | 100.05 | 99.41 | 99.73 | 99.60 | 99.87 | 99.41 | 100.07 | 99.4 | 99.8 | 99.8 | |
| A/CNK | 1.18 | 1.19 | 1.19 | 1.18 | 1.20 | 1.17 | 1.21 | 1.20 | 1.20 | 1.22 | 1.28 | 1.24 | 1.68 | 1.18 | 1.28 | 1.89 | 3.08 | 2.08 | 1.16 | |
| σ | 1.3 | 1.61 | 1.48 | 1.52 | 1.64 | 1.33 | 1.46 | 1.45 | 1.47 | 1.62 | 2.57 | 2.10 | 0.67 | 1.83 | 2.27 | 1.11 | 1.60 | 2.72 | 0.26 | |
| Cs | 16.09 | 15.81 | 15.08 | 16.46 | 15.66 | 15.41 | 18.48 | 21.4 | 20.54 | 6.758 | 6.606 | 6.111 | 7.952 | 8.633 | 3.801 | 13.98 | | | | |
| Sc | 8.63 | 8.57 | 8.82 | 9.34 | 8.21 | 8.74 | 7.87 | 8.97 | 9.01 | 5.248 | 4.79 | 5.288 | 8.654 | 7.05 | 4.742 | 11.02 | 8.6 | 12.7 | 8.2 | |
| Ba | 265.3 | 537.5 | 355.3 | 375.2 | 528.4 | 265.9 | 137.8 | 158 | 161.1 | 554 | 233.5 | 261.5 | 348.6 | 420.3 | 186.6 | 365.3 | 2444 | 861 | 167 | |
| Ti | 3111 | 2991 | 3099 | 3227 | 2943 | 3152 | 2805 | 3199 | 3197 | 1162 | 1060 | 1609 | 2326 | 1726 | 886 | 3035 | | | | |
| V | 65.63 | 62.42 | 64.44 | 68.62 | 61.47 | 68.25 | 59.56 | 70.73 | 71.16 | 21.01 | 11.52 | 16.08 | 49.19 | 33.81 | 5.373 | 65.27 | | | | |
| Mn | 794.7 | 616 | 697.2 | 741.6 | 595.6 | 805.7 | 735 | 843.1 | 867.5 | 550.6 | 569.3 | 514.7 | 820.9 | 853.4 | 685 | 609.3 | | | | |
| Co | 7.56 | 6.71 | 7.46 | 8.15 | 6.81 | 7.42 | 7.1 | 7.84 | 8.17 | 2.978 | 1.988 | 2.602 | 4.184 | 3.665 | 1.716 | 6.543 | | | | |
| Cr | 34.53 | 39.08 | 40.18 | 42.09 | 36.22 | 35.46 | 35.38 | 39.07 | 43.15 | 25.17 | 17.01 | 15.51 | 55.99 | 20.24 | 19.55 | 93.51 | 87 | 113 | 104 | |
| Ni | 14.39 | 13.76 | 16.06 | 17.69 | 11.27 | 15.77 | 13.98 | 17.04 | 17.58 | 8.146 | 4.041 | 5.023 | 15.69 | 7.365 | 2.744 | 28.03 | | | | |
| Cu | 11.65 | 11.72 | 9.98 | 11.03 | 9.74 | 13.54 | 21.8 | 22.94 | 23.3 | 10.79 | 13.87 | 6.321 | 20.68 | 69.59 | 11.59 | 39.9 | | | | |
| Zn | 72.73 | 67.74 | 73.78 | 68.7 | 58.77 | 73.07 | 72.84 | 74.53 | 79.71 | 35.22 | 67.78 | 162.8 | 56.08 | 44.47 | 35.19 | 48.82 | | | | |
| Pb | 18.99 | 24.22 | 20.06 | 17.21 | 21.33 | 17.78 | 10.84 | 12.84 | 12.59 | 18.35 | 51.73 | 60.64 | 3.916 | 11.7 | 35.89 | 2.738 | | | | |
| Ga | 20.1 | 19.53 | 19.43 | 18.84 | 18.42 | 19.97 | 17.94 | 19.93 | 20.17 | 12.58 | 16.74 | 18.56 | 17.63 | 19.19 | 18.07 | 19.31 | | | | |
| Ge | 1.67 | 1.84 | 1.7 | 1.73 | 1.73 | 1.57 | 2.01 | 1.08 | 1.47 | 1.699 | 1.486 | 1.927 | 1.984 | 1.876 | 1.603 | 2.364 | | | | |
| Rb | 183.9 | 177.1 | 157.9 | 169.7 | 177.5 | 163.1 | 152.5 | 171.8 | 171 | 173.1 | 274.1 | 225.6 | 185 | 227.2 | 267.2 | 256 | 216 | 243 | 80 | |
| Sr | 112.8 | 117.5 | 106.5 | 116.5 | 115.6 | 115.9 | 84.8 | 103.8 | 104.9 | 55.53 | 52.03 | 56.82 | 27.99 | 84.17 | 53.05 | 27.73 | 31 | 107 | 165 | |
| Hf | 1.63 | 1.48 | 1.12 | 1.46 | 5.59 | 0.41 | 1.51 | 1.53 | 2.14 | 3.584 | 2.174 | 4.099 | 4.802 | 3.778 | 1.808 | 2.688 | | | | |
| Zr | 61.75 | 60.43 | 61.6 | 62.45 | 66.07 | 57.39 | 62.17 | 68.63 | 81.44 | 124 | 65.13 | 128.8 | 159.4 | 123.5 | 50.05 | 89.02 | 190 | 118 | 579 | |

续表 2

Continued Table 2

| 样品号 | 5HI171 | 5HI172 | 5HI173 | 5HI174 | 5HI175 | 5HI176 | 5H031 | 5H032 | 5H033 | HT112 | HT51 | HT52 | HT54 | HT57 | HT60 | HT80 | G0103-1 | G0104-1 | G0105-1 | |
|-------------------------------------|--------|--------|--------|--------|--------|--------|-------|-------|-------|-------|--------|-------|-------|-------|-------|-------|---------|---------|---------|--|
| | 云楼岗岩体 | | | | | | | | | | 云开群混合岩 | | | | | | | | | |
| 岩性 | 云楼岗岩体 | | | | | | | | | | 云开群混合岩 | | | | | | | | | |
| Nb | 16.16 | 15.22 | 15.96 | 16.6 | 15.08 | 16.39 | 15.12 | 17.41 | 19.42 | 6.387 | 10.81 | 11.84 | 11.57 | 15.51 | 9.106 | 13.6 | 19 | 18 | 25 | |
| Ta | 1.82 | 1.24 | 1.57 | 1.44 | 1.49 | 1.51 | 1.2 | 1.58 | 4.52 | 1.429 | 1.273 | 1.13 | 1.255 | 1.383 | 0.562 | 1.687 | 28 | 26 | 33 | |
| Th | 14.66 | 13.87 | 14.27 | 15.57 | 14.65 | 14.92 | 12.12 | 14.39 | 14.02 | 6.071 | 6.987 | 19.99 | 14.5 | 13.01 | 5.126 | 15.63 | 19 | 19 | 46 | |
| U | 3.58 | 3.37 | 3.74 | 3.67 | 3.38 | 3.72 | 3.74 | 4.03 | 4.48 | 9.438 | 5.73 | 7.659 | 4.773 | 8.881 | 9.038 | 8.084 | 3.1 | 4.7 | 5.7 | |
| La | 31.02 | 27.25 | 25.33 | 31.02 | 27.14 | 31.67 | 23.12 | 26.51 | 29.98 | 12.29 | 13.34 | 30.88 | 27.28 | 27.62 | 7.603 | 35.25 | 63.27 | 52.52 | 82.74 | |
| Ce | 60.42 | 53.45 | 49.94 | 61.3 | 53.19 | 60.86 | 46.29 | 52.55 | 59.69 | 24.18 | 26.55 | 61.73 | 52.54 | 50.55 | 16.23 | 67.37 | 92.44 | 90.27 | 146.2 | |
| Pr | 7.46 | 6.71 | 6.19 | 7.61 | 6.68 | 7.52 | 5.88 | 6.53 | 7.46 | 2.999 | 3.231 | 7.548 | 6.343 | 5.922 | 2.079 | 8.12 | 10.87 | 8.98 | 13.86 | |
| Nd | 25.98 | 23.66 | 21.72 | 26.69 | 23.34 | 26.7 | 20.84 | 23.17 | 26.01 | 11.5 | 11.86 | 27.64 | 23.2 | 20.67 | 8.207 | 29.68 | 45.1 | 37.5 | 56.5 | |
| Sm | 5.02 | 4.54 | 4.12 | 5.07 | 4.51 | 5.1 | 4.06 | 4.5 | 5.1 | 2.529 | 2.472 | 5.159 | 4.264 | 3.887 | 2.392 | 5.535 | 8.85 | 7.44 | 10.5 | |
| Eu | 0.38 | 0.38 | 0.32 | 0.35 | 0.38 | 0.4 | 0.3 | 0.33 | 0.45 | 0.727 | 0.528 | 0.633 | 0.72 | 0.669 | 0.426 | 0.994 | 1.41 | 1.26 | 1.42 | |
| Gd | 5.08 | 4.56 | 4.15 | 5.06 | 4.61 | 5.16 | 4.02 | 4.58 | 5.31 | 2.505 | 2.15 | 4.007 | 3.781 | 3.343 | 2.711 | 4.955 | 7.55 | 6.91 | 10 | |
| Tb | 0.62 | 0.56 | 0.49 | 0.61 | 0.55 | 0.63 | 0.49 | 0.57 | 0.65 | 0.453 | 0.347 | 0.516 | 0.562 | 0.464 | 0.621 | 0.761 | 1.23 | 0.93 | 1.38 | |
| Dy | 2.84 | 2.55 | 2.31 | 2.71 | 2.57 | 2.94 | 2.31 | 2.72 | 3.02 | 2.774 | 2.009 | 2.56 | 3.198 | 2.28 | 3.97 | 4.463 | 6.14 | 5.7 | 7.27 | |
| Ho | 0.42 | 0.38 | 0.35 | 0.41 | 0.38 | 0.44 | 0.34 | 0.42 | 0.47 | 0.568 | 0.404 | 0.472 | 0.658 | 0.384 | 0.738 | 0.911 | 1.23 | 1.16 | 1.43 | |
| Er | 1.11 | 1.04 | 0.97 | 1.12 | 1.07 | 1.18 | 0.97 | 1.16 | 1.3 | 1.503 | 1.099 | 1.269 | 1.762 | 0.904 | 1.923 | 2.483 | 3.67 | 3.33 | 4.38 | |
| Tm | 0.1 | 0.09 | 0.08 | 0.09 | 0.09 | 0.1 | 0.08 | 0.1 | 0.12 | 0.224 | 0.177 | 0.191 | 0.263 | 0.131 | 0.286 | 0.375 | 0.48 | 0.47 | 0.6 | |
| Yb | 0.93 | 0.82 | 0.78 | 0.89 | 0.82 | 0.98 | 0.78 | 0.92 | 1.06 | 1.449 | 1.17 | 1.237 | 1.698 | 0.889 | 1.78 | 2.411 | 2.94 | 2.76 | 3.83 | |
| Lu | 0.09 | 0.07 | 0.07 | 0.08 | 0.07 | 0.09 | 0.07 | 0.09 | 0.11 | 0.226 | 0.179 | 0.192 | 0.273 | 0.142 | 0.255 | 0.376 | 0.45 | 0.49 | 0.69 | |
| Y | 12.62 | 11.38 | 10.24 | 12.08 | 11.51 | 12.22 | 10.64 | 11.41 | 13.24 | 14.07 | 10.63 | 11.88 | 15.98 | 9.605 | 20.85 | 23.17 | 28 | 26 | 33 | |
| ΣREE | 141.5 | 126.1 | 116.8 | 143 | 125.4 | 143.8 | 109.5 | 124.1 | 140.7 | 63.9 | 65.5 | 144.0 | 126.5 | 117.9 | 49.2 | 163.7 | 245.6 | 219.7 | 340.8 | |
| LREE | 130.3 | 116 | 107.6 | 132 | 115.2 | 132.3 | 100.5 | 113.6 | 128.7 | 54.2 | 58.0 | 133.6 | 114.3 | 109.3 | 36.9 | 146.9 | 221.9 | 198.0 | 311.2 | |
| HREE | 11.2 | 10.1 | 9.2 | 11 | 10.2 | 11.5 | 9.1 | 10.6 | 12 | 9.7 | 7.5 | 10.4 | 12.2 | 8.5 | 12.3 | 16.7 | 23.7 | 21.8 | 29.6 | |
| LREE/HREE | 11.6 | 11.5 | 11.7 | 12 | 11.3 | 11.5 | 11.1 | 10.8 | 10.7 | 5.6 | 7.7 | 12.8 | 9.4 | 12.8 | 3.0 | 8.8 | 9.4 | 9.1 | 10.5 | |
| (La/Yb) _N | 23.93 | 23.84 | 23.29 | 25.00 | 23.74 | 23.18 | 21.26 | 20.67 | 20.29 | 6.08 | 8.18 | 17.91 | 11.52 | 22.29 | 3.06 | 10.49 | 15.44 | 13.65 | 15.50 | |
| (La/Sm) _N | 3.99 | 3.87 | 3.97 | 3.95 | 3.88 | 4.01 | 3.68 | 3.80 | 3.79 | 3.14 | 3.48 | 3.86 | 4.13 | 4.59 | 2.05 | 4.11 | 4.62 | 4.56 | 5.09 | |
| δEu | 0.23 | 0.26 | 0.24 | 0.21 | 0.25 | 0.24 | 0.23 | 0.22 | 0.26 | 0.88 | 0.70 | 0.43 | 0.55 | 0.57 | 0.51 | 0.58 | 0.53 | 0.54 | 0.42 | |
| δCe | 1 | 1 | 0.97 | 0.97 | 0.98 | 0.98 | 0.97 | 0.97 | 0.97 | 0.98 | 0.99 | 0.99 | 0.98 | 0.97 | 1.00 | 0.98 | 0.86 | 1.02 | 1.06 | |
| Fe ₂ O ₃ /MgO | 2.65 | 2.56 | 2.60 | 2.57 | 2.55 | 2.64 | 2.66 | 2.70 | 2.65 | 3.20 | 3.99 | 4.24 | 2.51 | 3.14 | 6.14 | 2.65 | 5.38 | 2.33 | 4.04 | |
| 10000Ga/Al | 2.54 | 2.49 | 2.43 | 2.35 | 2.36 | 2.52 | 2.11 | 2.36 | 2.37 | 1.78 | 2.18 | 2.42 | 2.82 | 2.61 | 2.35 | 2.46 | | | | |
| Rb/Sr | 1.54 | 1.51 | 1.63 | 1.41 | 1.48 | 1.46 | 1.66 | 1.63 | 1.80 | 3.12 | 5.27 | 3.97 | 6.61 | 2.70 | 5.04 | 9.23 | 6.97 | 2.27 | 0.48 | |
| Nb/Ta | 8.88 | 12.27 | 10.17 | 11.53 | 10.12 | 10.85 | 12.60 | 11.02 | 4.30 | 4.47 | 8.49 | 10.48 | 9.22 | 11.21 | 16.20 | 8.06 | 0.68 | 0.69 | 0.76 | |

注:云开群变质沉积岩数据引自 Wan et al. (2010). $A/CNK = Al/(Ca + Na + K)$, $\delta Eu = Eu/Eu^* = Eu_N/(Sm_N \times Gd_N)^{1/2}$, $\delta Ce = Ce/Ce^* = Ce_N/(La_N \times Pr_N)^{1/2}$

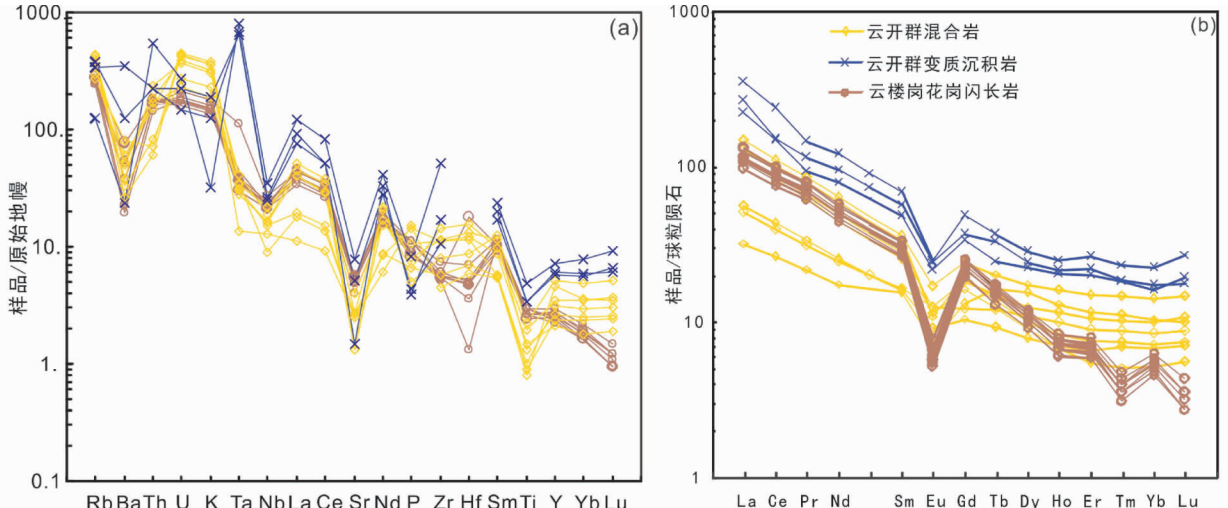


图7 全岩原始地幔标准化微量元素蛛网图(a, 标准化值据 Sun and McDonough, 1989)和球粒陨石标准化稀土元素配分图(b, 标准化值据 Boynton, 1984)

Fig.7 Primitive mantle-normalized trace element spidergrams (a, normalization values after Sun and McDonough, 1989) and chondrite-normalized REE diagrams (b, normalization values after Boynton, 1984)

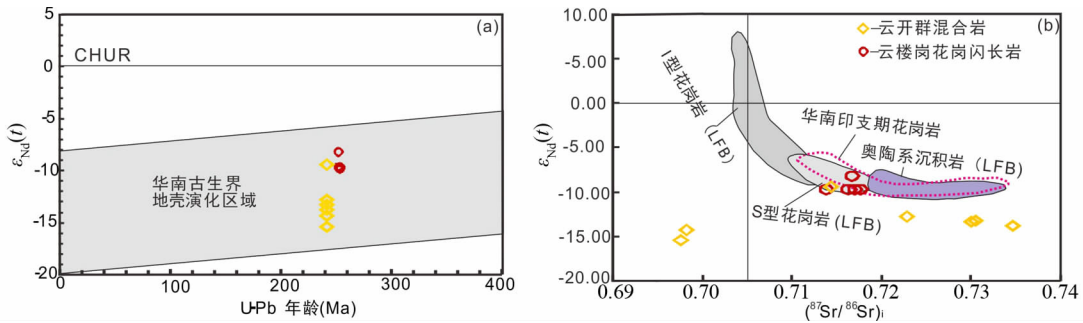


图8 云楼岗岩体和云开群混合岩 U-Pb 年龄-ε_{Nd}(t) 图解(a, 底图据周新民, 2007)和 (⁸⁷Sr/⁸⁶Sr)_i-ε_{Nd}(t) 图解(b, 底图据 Wang *et al.*, 2011)

LFB-东澳大利亚拉克兰褶皱带

Fig.8 Diagrams of U-Pb age vs. ε_{Nd}(t) (a, after Zhou, 2007) and (⁸⁷Sr/⁸⁶Sr)_i vs. ε_{Nd}(t) of the Yunlougang pluton and Yunkai Group migmatite (b, after Wang *et al.*, 2011)

LFB-Lachlan Fold Belt in east Australia

11.81% ~ 14.47% (图 6e), 与云楼岗岩体相近, 也是强过铝质的, A/CNK 为 1.18 ~ 1.89 (图 5b)。与云楼岗岩体相似, SiO₂ 与 TiO₂、Fe₂O₃^T、CaO、Al₂O₃、Nb 呈明显的负相关关系 (图 6a-e)。除了 2 个样品外, 其它也都属于高 K 钙碱性系列。在微量元素蛛网图上, Y、Yb 和 Lu 相对平坦, 而与云楼岗岩体类似, Ba、Nb、Sr、P 和 Ti 也强烈亏损 (图 7a)。混合岩的 ΣREE 含量变化较大, 为 49.2 × 10⁻⁶ ~ 163.7 × 10⁻⁶, 在稀土元素配分图上显示强烈的右倾特征 ((La/Yb)_N = 3.06 ~ 22.29, 平均 11.36), 轻稀土元素 LREE 也显示右倾特征 ((La/Sm)_N = 2.05 ~ 4.59), 而重稀土元素 HREE 则相对平坦 ((Ga/Yb)_N = 1.26 ~ 3.11) (图 7b)。类似于云楼岗岩体, 也具有明显的负 Eu 异常 (δEu = 0.43 ~ 0.88)。

4.3 全岩 Sr-Nd 同位素

表 3 为 5 个云楼岗岩体样品和 7 个云开群混合岩样品的 Sr-Nd 同位素测试结果。

云楼岗岩体的 ⁸⁷Sr/⁸⁶Sr 比值测试结果为 0.7309616 ~ 0.7324724。按照 253Ma 年龄计算岩体的初始 Sr-Nd 同位素组成, 计算结果为初始比值 (⁸⁷Sr/⁸⁶Sr)_i 为 0.71394 ~ 0.71773, ε_{Nd}(t) 为 -9.84 ~ -8.25 (图 8a), Nd 模式年龄为 1821 ~ 1692Ma。可见, 云楼岗岩体的 Sr-Nd 同位素组成与华南东部印支期 S 型花岗岩及东澳大利亚拉克兰褶皱带 (LFB) 的 Sr-Nd 同位素组成是基本一致的 (图 8b, Healy *et al.*, 2004; Wang *et al.*, 2011)。

表3 云楼岗岩体和云开群混合岩Sr-Nd同位素

Table 3 Sr-Nd isotopic composition of the Yunlougang pluton, the Yunlai Group migmatite and metasedimentary

| 样品号 | Sm ($\times 10^{-6}$) | Nd ($\times 10^{-6}$) | $\frac{^{147}\text{Sm}}{^{144}\text{Nd}}$ | $\frac{^{143}\text{Nd}}{^{144}\text{Nd}}$ | 2σ (Err.) | $\epsilon_{\text{Nd}}(t)$ | t_{DM2} (Ma) | Rb ($\times 10^{-6}$) | Sr ($\times 10^{-6}$) | $\frac{^{87}\text{Rb}}{^{86}\text{Sr}}$ | $\frac{^{87}\text{Sr}}{^{86}\text{Sr}}$ | 2σ (Err.) | $\left(\frac{^{87}\text{Sr}}{^{86}\text{Sr}}\right)_i$ |
|----------|----------------------------|----------------------------|---|---|---------------------|---------------------------|--------------------------|----------------------------|----------------------------|---|---|---------------------|--|
| 云楼岗岩体 | | | | | | | | | | | | | |
| 5H171 | 5.02 | 25.98 | 0.1168 | 0.512002 | 0.000006 | -12.41 | 1821 | 183.9 | 112.8 | 4.73 | 0.7309616 | 0.000007 | 0.71394 |
| 5H172 | 4.54 | 23.66 | 0.1160 | 0.512082 | 0.000005 | -10.86 | 1692 | 177.1 | 117.5 | 4.37 | 0.7324724 | 0.000011 | 0.71674 |
| 5H174 | 5.07 | 26.69 | 0.1148 | 0.512000 | 0.000004 | -12.44 | 1818 | 169.7 | 116.5 | 4.22 | 0.732312 | 0.000009 | 0.71711 |
| 5H175 | 4.51 | 23.34 | 0.1169 | 0.512004 | 0.000006 | -12.37 | 1818 | 177.5 | 115.6 | 4.45 | 0.7324125 | 0.000008 | 0.71639 |
| 5H176 | 5.10 | 26.70 | 0.1155 | 0.512000 | 0.000004 | -12.44 | 1819 | 163.1 | 115.9 | 4.08 | 0.7324125 | 0.000008 | 0.71773 |
| 云开群混合岩 | | | | | | | | | | | | | |
| HT112 | 2.53 | 11.50 | 0.1329 | 0.511829 | 0.000006 | -15.78 | 2133 | 173.1 | 55.5 | 9.07 | 0.7656535 | 0.000008 | 0.73469 |
| HT151 | 2.47 | 11.86 | 0.1260 | 0.511845 | 0.000008 | -15.47 | 2091 | 274.1 | 52.0 | 15.35 | 0.7829285 | 0.000011 | 0.73051 |
| HT152 | 5.16 | 27.64 | 0.1128 | 0.511821 | 0.000006 | -15.93 | 2096 | 225.6 | 56.8 | 11.56 | 0.7695157 | 0.000007 | 0.73006 |
| HT154 | 4.26 | 23.20 | 0.1111 | 0.511767 | 0.000005 | -17.00 | 2178 | 185.0 | 28.0 | 19.23 | 0.7638777 | 0.000011 | 0.69823 |
| HT157 | 3.89 | 20.67 | 0.1137 | 0.512021 | 0.000010 | -12.04 | 1783 | 227.2 | 84.2 | 7.84 | 0.7411494 | 0.000011 | 0.71440 |
| HT160 | 2.39 | 8.21 | 0.1762 | 0.511947 | 0.000009 | -13.49 | 2055 | 267.2 | 53.1 | 14.67 | 0.7729006 | 0.000011 | 0.72283 |
| HT180 | 5.54 | 29.68 | 0.1127 | 0.511714 | 0.000009 | -18.02 | 2264 | 256.0 | 27.7 | 26.93 | 0.7896009 | 0.000013 | 0.69768 |
| 云开群变质沉积岩 | | | | | | | | | | | | | |
| G0103-1 | 8.09 | 43.13 | 0.1134 | 0.511888 | 0.000008 | -14.60 | 1910 | | | | | | |
| G0104-1 | 7.08 | 37.08 | 0.1171 | 0.511772 | 0.000001 | -16.90 | 2170 | | | | | | |
| G0105-1 | 11.08 | 59.25 | 0.1131 | 0.511710 | 0.000012 | -18.10 | 2170 | | | | | | |

注:云开群变质沉积岩引自 Wan *et al.* (2010)

云开群混合岩的 $^{87}\text{Sr}/^{86}\text{Sr}$ 比值测试结果为0.7411494 ~ 0.7896009。基于240Ma年龄计算岩体的初始Sr-Nd同位素,初始比值($^{87}\text{Sr}/^{86}\text{Sr}$)_i为0.69768 ~ 0.73469, $\epsilon_{\text{Nd}}(t)$ 为-15.46 ~ -9.51(图8a),Nd模式年龄为2264 ~ 1783Ma。

4.4 黑云母成分

云楼岗岩体和云开群混合岩中的黑云母特征相似,都为棕红色叶片状,长0.5 ~ 3mm。表4为电子探针测试的黑云母化学成分和计算得到的离子含量。黑云母 Al^{IV} 和 $\text{Fe}^{\#}$ ($\text{Fe}^{\#} = \text{Fe}^{\text{T}} / (\text{Fe}^{\text{T}} + \text{Mg}^{2+})$)含量可以用来判断岩石的过铝质和氧化还原状态(Shabani *et al.*, 2003)。

云楼岗岩体中黑云母中 $\text{Fe}^{\#}$ 为0.48 ~ 0.52、 $\text{Mg}^{\#}$ 为0.48 ~ 0.53、 Al^{IV} 为2.612 ~ 2.758apfu(每个结构单元中的原子数)、 Ti^{4+} 为0.189 ~ 0.332apfu。在 $\text{Mg}-(\text{Fe}^{3+} + \text{Al}^{\text{VI}} + \text{Ti})-(\text{Fe}^{2+} + \text{Mn})$ 图上(图9a)显示为Mg质黑云母,而在 $10 \times \text{TiO}_2-(\text{FeO}^{\text{T}} + \text{MnO})-\text{MgO}$ 三角图解上(图9b)显示为受到改造再平衡的黑云母。利用黑云母中Ti(Henry *et al.*, 2005)和 Al^{T} 含量(Uchida *et al.*, 2007)可以作为地质温度计,计算得到的黑云母形成温度为589 ~ 679°C,平均651°C;压力为245 ~ 278MPa,平均266MPa;相当于9.27 ~ 10.51km,平均10.08km。

云开群混合岩中的黑云母与云楼岗岩体中的一样,也是Mg质的,并且是受到改造再平衡的黑云母(图9a, b),其中 $\text{Fe}^{\#}$ 、 $\text{Mg}^{\#}$ 值分别为0.44 ~ 0.56和0.44 ~ 0.56, Al^{IV} 和 Ti^{4+} 含量分别为2.663 ~ 2.880apfu和0.243 ~ 0.488apfu。计算得到形成温度为623 ~ 733°C,平均664°C;压力为211 ~ 323MPa,平均266MPa;相当于深度7.98 ~ 12.21km,平均10.06km。

5 讨论

5.1 云楼岗岩体与云开群混合岩的成因联系

受加里东构造运动作用,原始沉积的云开群在约440Ma时发生变质,形成低-中级变质相的变质沉积岩,例如板岩、片岩等(王孔忠等, 2006; Wang *et al.*, 2007a; Wan *et al.*, 2010)。根据地球化学特征,云楼岗花岗闪长岩及云开群混合岩可能都是云开群变质沉积岩在印支期局部再次受到强烈的改造而重熔的结果。云楼岗花岗闪长岩、云开群混合岩和云开群变质沉积岩三者具有许多类似的地球化学特征。它们都有高的 K_2O 含量、 $\text{Fe}_2\text{O}_3/\text{MgO}$ 比值(2.55 ~ 6.14)、以及Rb、Pb、LREE和初始($^{87}\text{Sr}/^{86}\text{Sr}$)_i比值,并且 $\epsilon_{\text{Nd}}(t)$ 都为负值,都具有低的10000Ga/Al比值,都亏损Ba、Nb、Sr、P和Ti, SiO_2 与 TiO_2 、 $\text{Fe}_2\text{O}_3^{\text{T}}$ 、CaO、Nb都具有负相关关系,这些特征表明它们都是壳源的(Whalen *et al.*, 1987; Jung *et al.*, 2000; Wang *et al.*, 2007a; Qiu *et al.*, 2014)。另外,云楼岗岩体与云开群混合岩中黑云母成分没有明显的区别,成因上都属于原生黑云母遭受改造形成的再平衡黑云母。说明形成两种岩石的熔体的熔融程度都很高,黑云母是从熔体中结

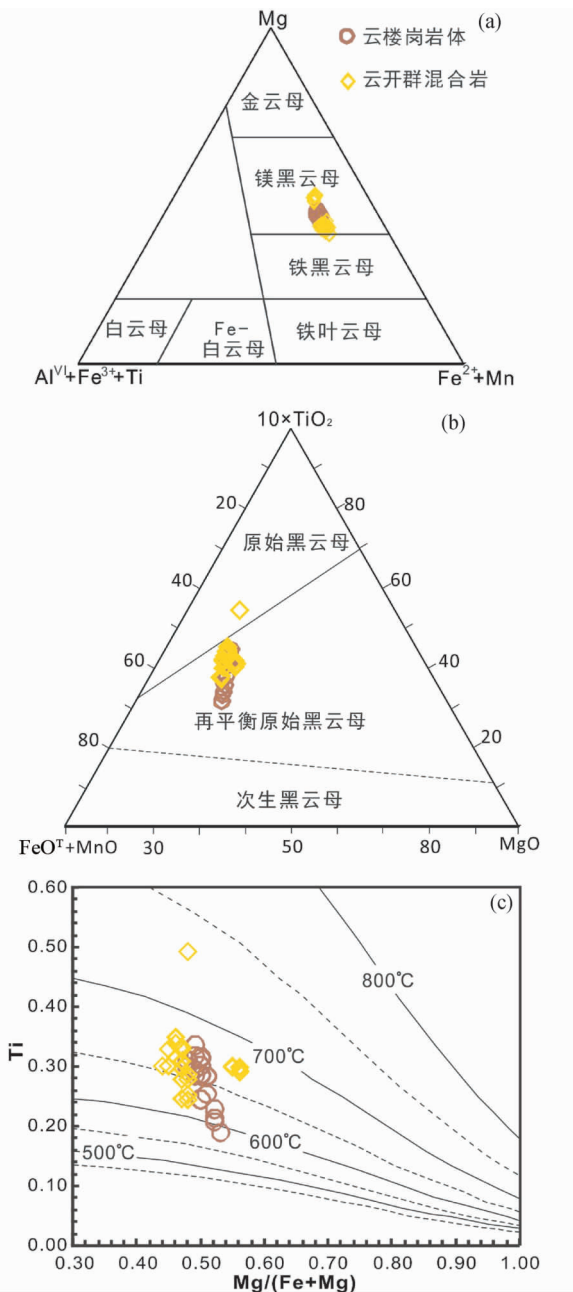


图9 黑云母 $Mg-(Fe^{2+} + Al^{VI} + Ti)-(Fe^{2+} + Mn)$ 分类图解(a, 底图据 Foster, 1960)、 $10 \times TiO_2-(FeO^T + MnO)-MgO$ 图解(b, 底图据 Nachit *et al.*, 2005) 和 $Ti-Mg/(Fe + Mg)$ 温压图解(c, 底图据 Henry *et al.*, 2005)

图9c中虚线为50°C间隔等温线

Fig. 9 Ternary $Mg-(Fe^{2+} + Mn)-(Al^{VI} + Fe^{3+} + Ti)$ (a, after Foster, 1960), ternary $10 \times TiO_2-(FeO^T + MnO)-MgO$ (b, after Nachit *et al.*, 2005) classification diagrams of biotites and Ti vs. $Mg/(Mg + Fe)$ diagram (c, after Henry *et al.*, 2005)

The dashed curves represent the intermediate 50°C interval isotherms in Fig. 9c

晶出来的原生黑云母,并且在后期都又遭受了改造。两种岩石中黑云母具有近乎相同的温度、压力和深度,反映了两者是在近乎相同的条件下遭受的改造。

然而,云楼岗岩体与云开群混合岩、变质沉积岩之间地球化学特征在许多方面也有区别。首先,云楼岗岩体的 SiO_2 含量比云开群混合岩要低。云开群混合岩的稀土配分曲线比较平,与云开群变质沉积岩形态类似,但是比较低(图7b)。云楼岗岩体的稀土配分曲线与之有较大差别,尽管轻稀土元素 LREE 与云开群变质沉积岩特征类似,但是重稀土元素则较曲折,不似云开群变质沉积岩那般平直。另外,云楼岗岩体的 $(La/Yb)_N$ 为 22.80,大于云开群变质沉积岩 $((La/Yb)_N = 14.86)$ 及混合岩 $((La/Yb)_N = 11.36)$,因此其稀土配分曲线整体斜率也更大。全岩 Rb/Sr 比可以作为指标用来判别熔体成因(Harris and Inger, 1992; Harris *et al.*, 1995; Solar and Brown, 2001)。云楼岗岩体的 Rb/Sr 比值相对较低,为 1.4 ~ 1.8,可能有外部岩浆的混入,使得云开群变质沉积岩发生重熔,并且由于混合岩岩浆熔融程度高, SiO_2 较低,从而导致 Rb/Sr 分馏程度较低。而云开群混合岩的 Rb/Sr 比值高,为 2.7 ~ 9.2,分馏程度高,说明云开群变质沉积岩中的云母发生了脱水熔融。当然,仅是云母脱水熔融不足以提供足够的熔体形成混合岩,推测可能还有其它外部流体的渗入导致水流熔融(Ward *et al.*, 2008; Sawyer *et al.*, 2011)。大陆地壳中产生水流熔融的许多地方都靠近主要剪切带,这些剪切带为含水流体渗入到大陆地壳中提供了通道(Sawyer, 2010)。云开地区存在着期左旋的剪切作用,时间在约 240Ma(Jiao *et al.*, 2017),与本文所得到的混合岩年龄一致,可以作为含水流体的通道使云开群变质沉积岩发生水流熔融。因此,总体来看,云开群混合岩的地球化学特征与云开群变质沉积岩更加类似,表明混合岩仅来自于变质沉积岩的直接熔融;而云楼岗岩体则有可能来自于混合岩浆,并且由于外部岩浆的加入,使得其 SiO_2 含量降低。另外,从 Sr-Nd 同位素特征来看,云楼岗岩体具有比云开群混合岩和变质沉积岩低的 $(^{87}Sr/^{86}Sr)_i$ 比值,高的 $\epsilon_{Nd}(t)$;前者的 Nd 模式年龄为 1821 ~ 1692Ma(平均 1794Ma),而后两者近乎一致为 2178 ~ 1783Ma(平均 2086Ma)和 2170 ~ 1910Ma(平均 2083Ma),前者明显小于后两者。当幔源的含水玄武岩侵入下地壳中时,能够形成一系列岩床,同时在地壳深部产生热区域,在这些热区域附近,由玄武岩不完全结晶残留下来的硅酸盐熔体可能与部分熔融的地壳岩石发生混合,从而形成混合硅酸盐熔体(Annen *et al.*, 2006)。这种混合而成的硅酸盐熔体可能具有闪长岩和花岗闪长岩的成分(Suga *et al.*, 2016)。因此,在形成云楼岗花岗闪长岩体时,可能有来自地幔的年轻熔体成分加入到局部重熔的下地壳的熔体中从而形成混合岩浆。Jiao *et al.* (2015)对云开地区的大容山 S 型花岗岩杂岩体的成因进行了详细研究,研究表明其形成于约 249Ma,同样也是混合岩浆结晶形成的,有少量地幔物质的加入,与云楼岗岩体具有类似的成因,可见其成因在区域上有

表 4 云楼岗岩体和云开群混合黑云母化学组成 (wt%)

Table 4 Geochemical composition of the biotites in the Yunlonggang pluton and the Yunkai Group migmatite (wt%)

| 测点号 | (wt%) | | | | | | | | | | | (apuf) | | | | | | Mg [#] | T (°C) | P (MPa) | H (km) | | |
|----------|------------------|------------------|--------------------------------|-------|------|-------|-------------------|------------------|------------------|-------|------------------|------------------|------------------|------------------|------------------|------------------|------------------|-----------------|-----------|------------|-----------|------------------|-----------------|
| | SiO ₂ | TiO ₂ | Al ₂ O ₃ | FeO | MnO | MgO | Na ₂ O | K ₂ O | H ₂ O | Total | Si ⁴⁺ | Al ^{IV} | Al ^{VI} | Ti ⁴⁺ | Fe ³⁺ | Fe ²⁺ | Mn ²⁺ | | | | | Mg ²⁺ | Fe [#] |
| 云楼岗岩体 | | | | | | | | | | | | | | | | | | | | | | | |
| 5H031-1 | 36.67 | 2.87 | 17.68 | 18.04 | 0.35 | 9.96 | 0.08 | 9.09 | 2.07 | 96.81 | 5.309 | 2.691 | 0.324 | 0.313 | 0.176 | 2.008 | 0.042 | 2.149 | 0.5 | 0.5 | 672.5 | 260.5 | 9.85 |
| 5H031-2 | 36.87 | 2.62 | 17.60 | 18.15 | 0.35 | 10.08 | 0.06 | 9.24 | 2.07 | 97.04 | 5.33 | 2.67 | 0.326 | 0.285 | 0.181 | 2.013 | 0.043 | 2.173 | 0.5 | 0.5 | 657.3 | 254.8 | 9.63 |
| 5H031-3 | 36.18 | 3.04 | 17.77 | 18.24 | 0.33 | 9.98 | 0.10 | 9.51 | 2.07 | 97.21 | 5.242 | 2.758 | 0.275 | 0.332 | 0.169 | 2.042 | 0.041 | 2.155 | 0.51 | 0.49 | 679.8 | 266.0 | 10.05 |
| 5H031-4 | 36.60 | 2.73 | 17.67 | 17.91 | 0.35 | 10.02 | 0.04 | 9.39 | 2.07 | 96.79 | 5.308 | 2.692 | 0.326 | 0.298 | 0.174 | 1.998 | 0.043 | 2.167 | 0.5 | 0.5 | 664.6 | 261.5 | 9.88 |
| 5H031-5 | 36.56 | 2.22 | 17.90 | 18.39 | 0.29 | 10.14 | 0.08 | 9.34 | 2.07 | 96.99 | 5.299 | 2.701 | 0.355 | 0.242 | 0.172 | 2.057 | 0.035 | 2.191 | 0.5 | 0.5 | 629.0 | 273.0 | 10.32 |
| 5H031-6 | 36.28 | 2.84 | 17.87 | 18.71 | 0.34 | 9.74 | 0.08 | 9.29 | 2.07 | 97.21 | 5.259 | 2.741 | 0.309 | 0.309 | 0.173 | 2.095 | 0.041 | 2.106 | 0.52 | 0.48 | 666.5 | 271.2 | 10.25 |
| 5H031-7 | 35.95 | 2.84 | 17.59 | 17.96 | 0.31 | 9.70 | 0.08 | 9.02 | 2.04 | 95.50 | 5.285 | 2.715 | 0.331 | 0.314 | 0.171 | 2.036 | 0.038 | 2.125 | 0.51 | 0.49 | 671.0 | 269.9 | 10.20 |
| 5H031-8 | 36.45 | 2.69 | 17.89 | 18.48 | 0.33 | 9.91 | 0.06 | 9.50 | 2.07 | 97.38 | 5.271 | 2.729 | 0.318 | 0.293 | 0.172 | 2.063 | 0.04 | 2.137 | 0.51 | 0.49 | 659.8 | 270.2 | 10.21 |
| 5H031-9 | 36.35 | 2.82 | 17.70 | 18.38 | 0.40 | 9.52 | 0.09 | 9.13 | 2.06 | 96.46 | 5.299 | 2.701 | 0.338 | 0.309 | 0.176 | 2.065 | 0.05 | 2.069 | 0.52 | 0.48 | 666.5 | 267.8 | 10.12 |
| 5H031-10 | 36.20 | 2.74 | 17.96 | 18.83 | 0.37 | 9.70 | 0.08 | 9.03 | 2.07 | 96.98 | 5.256 | 2.744 | 0.327 | 0.299 | 0.171 | 2.115 | 0.046 | 2.1 | 0.52 | 0.48 | 661.1 | 277.5 | 10.49 |
| 5H031-11 | 36.76 | 2.59 | 17.32 | 18.26 | 0.35 | 10.02 | 0.08 | 9.21 | 2.06 | 96.65 | 5.343 | 2.657 | 0.308 | 0.283 | 0.190 | 2.029 | 0.043 | 2.171 | 0.51 | 0.49 | 654.0 | 245.4 | 9.27 |
| 5H031-12 | 36.51 | 2.83 | 17.66 | 17.69 | 0.33 | 9.94 | 0.09 | 9.27 | 2.06 | 96.38 | 5.31 | 2.69 | 0.334 | 0.31 | 0.172 | 1.979 | 0.041 | 2.155 | 0.5 | 0.5 | 671.0 | 263.3 | 9.95 |
| 5H031-13 | 36.33 | 2.84 | 17.52 | 17.71 | 0.32 | 9.89 | 0.09 | 9.26 | 2.05 | 95.98 | 5.309 | 2.691 | 0.324 | 0.312 | 0.174 | 1.990 | 0.039 | 2.154 | 0.5 | 0.5 | 672.0 | 260.5 | 9.85 |
| 5H031-14 | 36.49 | 2.87 | 17.81 | 18.03 | 0.34 | 9.97 | 0.09 | 9.27 | 2.07 | 96.94 | 5.284 | 2.716 | 0.322 | 0.312 | 0.170 | 2.014 | 0.041 | 2.153 | 0.5 | 0.5 | 672.0 | 267.5 | 10.11 |
| 5H171-1 | 37.11 | 1.73 | 17.70 | 17.09 | 0.32 | 10.60 | 0.04 | 9.57 | 2.07 | 96.24 | 5.388 | 2.612 | 0.414 | 0.189 | 0.172 | 1.903 | 0.04 | 2.295 | 0.47 | 0.53 | 589.2 | 263.9 | 9.97 |
| 5H171-2 | 36.42 | 1.94 | 17.67 | 17.22 | 0.36 | 10.54 | 0.13 | 9.39 | 2.05 | 95.71 | 5.327 | 2.673 | 0.371 | 0.213 | 0.167 | 1.939 | 0.044 | 2.297 | 0.48 | 0.52 | 610.2 | 269.3 | 10.18 |
| 5H171-3 | 36.27 | 2.61 | 17.94 | 18.24 | 0.34 | 10.22 | 0.07 | 9.85 | 2.07 | 97.60 | 5.242 | 2.758 | 0.295 | 0.283 | 0.166 | 2.038 | 0.041 | 2.201 | 0.5 | 0.5 | 656.2 | 272.1 | 10.28 |
| 5H171-4 | 36.66 | 2.62 | 18.04 | 17.92 | 0.29 | 10.28 | 0.06 | 9.75 | 2.08 | 97.70 | 5.274 | 2.726 | 0.33 | 0.283 | 0.164 | 1.991 | 0.035 | 2.204 | 0.49 | 0.51 | 658.4 | 273.0 | 10.32 |
| 5H171-5 | 37.21 | 2.09 | 17.92 | 17.22 | 0.29 | 10.47 | 0.06 | 9.63 | 2.08 | 96.96 | 5.363 | 2.637 | 0.404 | 0.226 | 0.168 | 1.907 | 0.035 | 2.249 | 0.48 | 0.52 | 621.4 | 268.4 | 10.14 |
| 5H171-6 | 35.40 | 2.47 | 17.03 | 16.46 | 0.29 | 9.70 | 0.06 | 9.52 | 1.99 | 92.93 | 5.338 | 2.662 | 0.363 | 0.28 | 0.168 | 1.908 | 0.037 | 2.18 | 0.49 | 0.51 | 656.6 | 263.6 | 9.96 |
| 5H171-7 | 36.28 | 2.31 | 17.83 | 17.65 | 0.34 | 10.35 | 0.09 | 9.55 | 2.06 | 96.47 | 5.282 | 2.718 | 0.34 | 0.253 | 0.164 | 1.986 | 0.042 | 2.247 | 0.49 | 0.51 | 639.3 | 273.6 | 10.34 |
| 5H171-8 | 36.69 | 1.89 | 17.95 | 17.40 | 0.27 | 10.47 | 0.10 | 9.40 | 2.06 | 96.22 | 5.333 | 2.667 | 0.406 | 0.207 | 0.164 | 1.951 | 0.033 | 2.269 | 0.48 | 0.52 | 604.6 | 278.1 | 10.51 |
| 平均 | 36.47 | 2.55 | 17.73 | 17.91 | 0.33 | 10.05 | 0.08 | 9.37 | 2.06 | 96.55 | 5.302 | 2.698 | 0.338 | 0.279 | 0.171 | 2.006 | 0.040 | 2.179 | 0.50 | 0.50 | 651.5 | 266.9 | 10.09 |
| 云开群混合岩 | | | | | | | | | | | | | | | | | | | | | | | |
| HT104-1 | 35.80 | 2.80 | 18.45 | 18.67 | 0.18 | 9.13 | 0.14 | 9.50 | 2.06 | 96.73 | 5.221 | 2.779 | 0.39 | 0.307 | 0.155 | 2.122 | 0.022 | 1.984 | 0.53 | 0.47 | 663.5 | 307.2 | 11.61 |
| HT104-2 | 35.71 | 2.52 | 18.11 | 18.51 | 0.18 | 9.61 | 0.08 | 9.45 | 2.05 | 96.22 | 5.233 | 2.767 | 0.359 | 0.277 | 0.160 | 2.108 | 0.023 | 2.1 | 0.52 | 0.48 | 648.3 | 294.2 | 11.12 |
| HT104-3 | 35.20 | 2.26 | 18.54 | 18.76 | 0.17 | 9.54 | 0.11 | 9.53 | 2.04 | 96.15 | 5.176 | 2.824 | 0.386 | 0.25 | 0.149 | 2.158 | 0.022 | 2.091 | 0.52 | 0.48 | 630.4 | 319.6 | 12.08 |

续表 4
Continued Table 4

| 测点号 | (wt%) | | | | | | | | | | | (apuf) | | | | | | | Fe [#] | Mg [#] | T (°C) | P (MPa) | H (km) |
|---------|------------------|------------------|--------------------------------|-------|------|-------|-------------------|------------------|------------------|-------|------------------|------------------|------------------|------------------|------------------|------------------|------------------|------------------|-----------------|-----------------|--------|---------|--------|
| | SiO ₂ | TiO ₂ | Al ₂ O ₃ | FeO | MnO | MgO | Na ₂ O | K ₂ O | H ₂ O | Total | Si ⁴⁺ | Al ^{IV} | Al ^{VI} | Ti ⁴⁺ | Fe ³⁺ | Fe ²⁺ | Mn ²⁺ | Mg ²⁺ | | | | | |
| HT104-4 | 35.00 | 2.17 | 17.94 | 18.23 | 0.16 | 9.18 | 0.10 | 9.32 | 2.00 | 94.09 | 5.244 | 2.756 | 0.409 | 0.244 | 0.157 | 2.127 | 0.02 | 2.05 | 0.53 | 0.47 | 623.8 | 306.0 | 11.56 |
| HT104-5 | 35.65 | 2.27 | 18.70 | 18.40 | 0.19 | 9.38 | 0.15 | 9.53 | 2.05 | 96.31 | 5.216 | 2.784 | 0.438 | 0.25 | 0.147 | 2.105 | 0.024 | 2.046 | 0.52 | 0.48 | 630.4 | 323.3 | 12.22 |
| HT104-6 | 34.89 | 4.42 | 17.65 | 18.39 | 0.16 | 9.43 | 0.13 | 9.05 | 2.04 | 96.15 | 5.12 | 2.88 | 0.17 | 0.488 | 0.161 | 2.096 | 0.02 | 2.063 | 0.52 | 0.48 | 733.3 | 271.2 | 10.25 |
| HT104-7 | 35.57 | 2.51 | 18.30 | 18.86 | 0.19 | 9.50 | 0.05 | 9.38 | 2.05 | 96.40 | 5.209 | 2.791 | 0.365 | 0.276 | 0.158 | 2.151 | 0.023 | 2.073 | 0.53 | 0.47 | 645.7 | 303.3 | 11.46 |
| HT104-8 | 35.38 | 2.56 | 17.27 | 18.89 | 0.15 | 9.69 | 0.07 | 9.32 | 2.02 | 95.34 | 5.25 | 2.75 | 0.268 | 0.285 | 0.183 | 2.161 | 0.018 | 2.143 | 0.52 | 0.48 | 653.2 | 261.5 | 9.88 |
| HT104-9 | 35.26 | 2.19 | 18.47 | 18.45 | 0.19 | 9.44 | 0.15 | 9.36 | 2.03 | 95.53 | 5.206 | 2.794 | 0.418 | 0.243 | 0.149 | 2.129 | 0.023 | 2.077 | 0.52 | 0.48 | 625.2 | 320.2 | 12.10 |
| HT13-1 | 36.31 | 3.04 | 16.48 | 19.41 | 0.26 | 9.34 | 0.07 | 9.64 | 2.04 | 96.58 | 5.335 | 2.665 | 0.187 | 0.336 | 0.227 | 2.158 | 0.032 | 2.045 | 0.54 | 0.46 | 676.2 | 211.2 | 7.98 |
| HT13-2 | 36.21 | 2.83 | 17.02 | 19.36 | 0.28 | 9.25 | 0.06 | 9.64 | 2.04 | 96.68 | 5.311 | 2.689 | 0.251 | 0.312 | 0.205 | 2.170 | 0.034 | 2.023 | 0.54 | 0.46 | 664.3 | 237.8 | 8.99 |
| HT13-3 | 36.26 | 2.96 | 17.13 | 18.93 | 0.20 | 9.30 | 0.06 | 9.71 | 2.05 | 96.59 | 5.311 | 2.689 | 0.265 | 0.326 | 0.197 | 2.122 | 0.024 | 2.031 | 0.53 | 0.47 | 673.2 | 242.1 | 9.15 |
| HT13-4 | 36.29 | 2.95 | 16.59 | 19.24 | 0.22 | 9.38 | 0.06 | 9.72 | 2.04 | 96.50 | 5.334 | 2.666 | 0.206 | 0.326 | 0.221 | 2.144 | 0.027 | 2.056 | 0.53 | 0.47 | 673.2 | 217.2 | 8.21 |
| HT13-5 | 36.27 | 2.97 | 17.20 | 18.90 | 0.27 | 9.38 | 0.08 | 9.68 | 2.05 | 96.78 | 5.301 | 2.699 | 0.261 | 0.326 | 0.194 | 2.117 | 0.033 | 2.043 | 0.53 | 0.47 | 673.2 | 243.9 | 9.22 |
| HT13-6 | 35.83 | 2.71 | 17.83 | 20.37 | 0.27 | 8.96 | 0.05 | 8.97 | 2.05 | 97.04 | 5.238 | 2.762 | 0.308 | 0.298 | 0.185 | 2.305 | 0.033 | 1.952 | 0.56 | 0.44 | 653.3 | 277.2 | 10.48 |
| HT13-7 | 36.57 | 2.74 | 17.62 | 19.56 | 0.27 | 9.01 | 0.07 | 9.74 | 2.07 | 97.64 | 5.308 | 2.692 | 0.319 | 0.299 | 0.191 | 2.183 | 0.033 | 1.949 | 0.55 | 0.45 | 655.6 | 259.3 | 9.80 |
| HT13-8 | 35.11 | 2.85 | 16.26 | 18.75 | 0.20 | 8.75 | 0.05 | 9.22 | 1.97 | 93.16 | 5.337 | 2.663 | 0.247 | 0.326 | 0.214 | 2.170 | 0.026 | 1.984 | 0.55 | 0.45 | 669.7 | 228.7 | 8.64 |
| HT13-9 | 35.82 | 2.65 | 17.01 | 18.71 | 0.26 | 9.28 | 0.07 | 9.49 | 2.02 | 95.31 | 5.315 | 2.685 | 0.288 | 0.295 | 0.194 | 2.128 | 0.033 | 2.052 | 0.53 | 0.47 | 657.0 | 247.8 | 9.37 |
| HT13-10 | 35.75 | 3.14 | 17.06 | 19.75 | 0.26 | 9.32 | 0.08 | 9.23 | 2.04 | 96.63 | 5.251 | 2.749 | 0.202 | 0.347 | 0.201 | 2.224 | 0.033 | 2.04 | 0.54 | 0.46 | 681.2 | 241.2 | 9.11 |
| HT13-11 | 36.20 | 3.01 | 17.06 | 19.22 | 0.19 | 9.45 | 0.10 | 9.53 | 2.05 | 96.81 | 5.293 | 2.707 | 0.231 | 0.331 | 0.201 | 2.149 | 0.024 | 2.061 | 0.53 | 0.47 | 675.6 | 237.2 | 8.97 |
| HT13-12 | 36.14 | 2.95 | 17.02 | 19.62 | 0.28 | 9.11 | 0.04 | 9.65 | 2.05 | 96.86 | 5.299 | 2.701 | 0.237 | 0.326 | 0.206 | 2.199 | 0.035 | 1.991 | 0.55 | 0.45 | 669.7 | 237.2 | 8.97 |
| HT5-1 | 36.60 | 2.69 | 18.01 | 16.45 | 0.16 | 11.67 | 0.07 | 10.06 | 2.10 | 97.81 | 5.233 | 2.767 | 0.266 | 0.289 | 0.150 | 1.817 | 0.019 | 2.487 | 0.44 | 0.56 | 673.7 | 266.0 | 10.05 |
| HT5-2 | 36.56 | 2.75 | 17.57 | 16.61 | 0.15 | 11.80 | 0.11 | 9.69 | 2.09 | 97.32 | 5.25 | 2.75 | 0.221 | 0.297 | 0.162 | 1.833 | 0.018 | 2.526 | 0.44 | 0.56 | 678.0 | 247.2 | 9.34 |
| HT5-3 | 36.66 | 2.70 | 17.89 | 16.63 | 0.15 | 11.89 | 0.09 | 9.99 | 2.10 | 98.10 | 5.228 | 2.772 | 0.233 | 0.29 | 0.155 | 1.829 | 0.019 | 2.527 | 0.44 | 0.56 | 674.3 | 257.5 | 9.73 |
| HT5-4 | 36.49 | 2.77 | 18.39 | 16.37 | 0.13 | 11.82 | 0.10 | 9.90 | 2.11 | 98.07 | 5.195 | 2.805 | 0.278 | 0.296 | 0.140 | 1.809 | 0.016 | 2.509 | 0.44 | 0.56 | 677.5 | 281.1 | 10.63 |
| HT5-5 | 36.74 | 2.79 | 18.41 | 16.60 | 0.17 | 11.40 | 0.09 | 10.06 | 2.11 | 98.36 | 5.222 | 2.778 | 0.303 | 0.299 | 0.144 | 1.829 | 0.02 | 2.415 | 0.45 | 0.55 | 676.6 | 280.5 | 10.60 |
| HT5-6 | 36.31 | 2.73 | 17.85 | 16.27 | 0.18 | 11.21 | 0.10 | 9.82 | 2.07 | 96.54 | 5.254 | 2.746 | 0.295 | 0.297 | 0.151 | 1.818 | 0.022 | 2.418 | 0.45 | 0.55 | 675.5 | 268.4 | 10.14 |
| 平均 | 35.95 | 2.77 | 17.62 | 18.44 | 0.20 | 9.82 | 0.08 | 9.56 | 2.05 | 96.51 | 5.255 | 2.745 | 0.289 | 0.305 | 0.176 | 2.080 | 0.025 | 2.138 | 0.51 | 0.49 | 664.1 | 266.2 | 10.06 |

注: 结构式以 22 个氧原子进行计算. $Fe^{\#} = Fe^{\text{IV}} / (Fe^{\text{IV}} + Mg^{2+})$; $Mg^{\#} = Mg^{2+} / (Fe^{\text{IV}} + Mg^{2+})$; 温度 $T = [\ln(\bar{\Gamma}) - a - c(XMg)^3] / b^{0.333}$ (Henry *et al.*, 2005); 压力 $P = [3.03 \times T^{\text{Al}} - 6.53 (\pm 0.33)] \times 100$ (Uehida *et al.*, 2007); 深度 $H = P / \rho g$, $\rho = 2700 \text{ kg/m}^3$, $g = 9.8 \text{ m/s}^2$

一定的普遍性。而云开群混合岩与变质沉积岩有近乎一致的 Sr-Nd 同位素特征及 Nd 模式年龄,因此,云开群混合岩是变质沉积岩部分熔融并在原地结晶形成的,没有明显的外部熔体(地幔物质)的混入。

从地质年代学上看,前人曾在云开群局部变质程度较高的片麻岩中获得 242 ~ 236Ma 的印支期变质重置年龄(Wang *et al.*, 2007a; Wan *et al.*, 2010),与本文获得的云开群混合岩的 U-Pb 年龄 240.3 ± 5.1 Ma 近乎一致,可见,云开地区在印支期发生过一次广泛的构造热事件。然而,云楼岗岩体的年龄是 253 ± 1.6 Ma,在分析误差范围内比混合岩中变质锆石的年龄早了 10Myr,因此,云楼岗岩体并非附近云开群混合岩化的产物,与河台矿区的混合岩也不是同源的。

5.2 大地构造意义

印支期造山运动奠定了中国东部的构造格局,对于区域构造发展、岩浆活动及变质作用有重要的影响(Huang *et al.*, 1987; Ren, 1991, 1996; Wang *et al.*, 2007a)。在华南板块印支期过铝质花岗岩以大规模的岩盖及广泛分布的小型侵入体形式产出,分布面积约 21000km²,约占整个华南花岗岩的 12.3% (图 1a; 湖南省地质矿产局, 1988; 孙涛, 2006; Mao *et al.*, 2011)。其中包括 60% 强过铝质 ($A/CNK > 1.1$) S-型花岗岩露头,30% 的弱过铝质 ($A/CNK = 1.0 \sim 1.1$) 和 10% 的钙碱性 I 型花岗岩(邓希光等, 2004; Sun *et al.*, 2005; Qiu *et al.*, 2014)。然而,由于出露的印支期花岗岩年龄范围较广,在约 260 ~ 210Ma 都有产出(Chu *et al.*, 2012a, b; Wang *et al.*, 2007a, 2013; Qiu *et al.*, 2014),使得印支期构造岩浆事件的时空分布格局及终结时间存在争议(Wang *et al.*, 2013)。华南板块位于两大碰撞造山带之间,北部与华北板块之间为大别苏鲁超高压变质带,西南与印支板块之间为宋马带(图 1a)。由于位于这些造山带之间,华南板块在印支期整体处于压缩环境,并且广泛发育印支期花岗岩。华南板块西南部大量的花岗岩形成在 258 ~ 242Ma,可能主要与古特提斯洋的闭合导致印支板块北部与华南板块的陆陆碰撞有关(Nam *et al.*, 1998; Carter *et al.*, 2001; Wang *et al.*, 2010);而华南板块与华北板块碰撞的时间相对较晚,因此华南板块北部花岗岩多为 240 ~ 225Ma(Li *et al.*, 1993; Zheng, 2008; Zhao *et al.*, 2013)。

在河台地区,印支期岩浆岩、混合岩和韧性剪切带并存,说明它们与造山活动有密切关系(Solar and Brown, 2001; Johannes *et al.*, 2003; Sepahi *et al.*, 2013)。但三者的形成时间又有所不同,可能代表造山作用不同演化阶段的产物。云楼岗岩体的侵入(约 253Ma)和云开群混合岩的形成(约 240Ma)可能都与古特提斯洋的闭合以及华南板块与印支板块之间的陆陆碰撞有关,但是岩浆作用的时间却比混合岩化的时间早了 10Myr。云楼岗岩体形成在 253Ma 的同碰撞压缩条件下,地壳加厚导致下地壳岩石局部发生深熔,并且有少量年轻的地幔物质加入。随后,在 240Ma 随着造山带的坍塌

剥蚀,导致云开地区地壳降压熔融从而形成混合岩(Wang *et al.*, 2012)。而此时,在空间上岩浆岩则出现在广东中部,甚至更东部的湖南江西一带(图 1a)。可见,碰撞对华南板块的影响随时间逐渐向东迁移。前人研究表明,河台地区剪切带的形成时间有两期,早期为左旋,发生在约 240Ma,晚期为右旋,发生在约 204Ma(Jiao *et al.*, 2017)。混合岩化的发生时间与早期左旋运动的时间大致相当。这些剪切带和混合岩代表了碰撞晚期的逆冲走滑作用和变质沉积岩的降压熔融(Wang *et al.*, 2007b, 2012)。综上所述,云开地区印支期的花岗岩可能是华南板块和印支板块碰撞高峰期的作用产物,而云开群混合岩和韧性剪切带则可能是终了期的产物。

6 结论

(1) 云楼岗花岗岩闪长岩体与邻近的云开群混合岩不是同源的,不是混合岩化的最终产物。岩体可能是地壳深熔并有少量年轻的地幔物质混入形成的混合岩浆结晶而成。而云开群混合岩则可能仅是云开群变质沉积岩原地熔融形成的。

(2) 云楼岗岩体的形成时间是约 253Ma,云开群局部混合岩化的时间是约 240Ma,可能分别代表的是华南板块和印支板块碰撞高峰期和终了期的产物。

References

- Andersen T. 2002. Correction of common lead in U-Pb analyses that do not report ²⁰⁴Pb. *Chemical Geology*, 192(1-2): 59-79
- Annen C, Blundy JD and Sparks RSJ. 2006. The genesis of intermediate and silicic magmas in deep crustal hot zones. *Journal of Petrology*, 47(3): 505-539
- Black LP, Kamo SL, Williams IS, Mundil R, Davis DW, Korsch RJ and Foudoulis C. 2003. The application of SHRIMP to Phanerozoic geochronology: A critical appraisal of four zircon standards. *Chemical Geology*, 200(1-2): 171-188
- Boynnton WV. 1984. Geochemistry of the rare earth elements; Meteorite studies. In: Henderson P (ed.). *Rare Earth Element Geochemistry*. Amsterdam: Elsevier, 63-114
- Brown M. 1994. The generation, segregation, ascent and emplacement of granite magma: The migmatite-to-crustally-derived granite connection in thickened orogens. *Earth-Science Reviews*, 36(1-2): 83-130
- Brown M, Averkin YA, McLellan EL and Sawyer EW. 1995. Melt segregation in migmatites. *Journal of Geophysical Research*, 100(B8): 15655-15679
- Brown M. 2007. Crustal melting and melt extraction, ascent and emplacement in orogens: Mechanisms and consequences. *Journal of the Geological Society*, 164(4): 709-730
- Bureau of Geology and Mineral Resources of Guangxi Zhuang Autonomous Region. 1985. *Regional Geology of Guangxi Zhuang Autonomous Region*. Beijing: Geological Publishing House (in Chinese)
- Bureau of Geology and Mineral Resources of Hunan Province. 1988. *Regional Geology of Hunan Province*. Beijing: Geological Publishing House (in Chinese)
- Cai MH, Zhan MG, Peng SB, Meng XJ and Liu GQ. 2002. Study of Mesozoic metallogenic geological setting and dynamic mechanism in Yunkai area. *Mineral Deposits*, 21(3): 264-269 (in Chinese with English abstract)

- Carter A, Roques D, Bristow C and Kinny P. 2001. Understanding Mesozoic accretion in Southeast Asia: Significance of Triassic thermotectonism (Indosinian orogeny) in Vietnam. *Geology*, 29 (3): 211–214
- Chappell BW and White AJR. 1992. I- and S-type granites in the Lachlan Fold Belt. *Earth and Environmental Science Transactions of the Royal Society of Edinburgh*, 83(1–2): 1–26
- Chappell BW. 1999. Aluminium saturation in I- and S-type granites and the characterization of fractionated haplogranites. *Lithos*, 46 (3): 535–551
- Chen CH, Hsieh PS, Lee CY and Zhou HW. 2011. Two episodes of the Indosinian thermal event on the South China Block: Constraints from LA-ICP MS U-Pb zircon and electron microprobe monazite ages of the Darongshan S-type granitic suite. *Gondwana Research*, 19 (4): 1008–1023
- Chen CH, Liu YH, Lee CY, Xiang H and Zhou HW. 2012. Geochronology of granulite, charnockite and gneiss in the poly-metamorphosed Gaozhou Complex (Yunkai massif), South China: Emphasis on the in-situ EMP monazite dating. *Lithos*, 144–145: 109–129
- Chen J and Wang HN. 1993. Characteristics of REE and other trace elements within a shear zone of the Hetai gold deposit, Guangdong Province. *Mineral Deposits*, 12 (3): 202–211 (in Chinese with English abstract)
- Chu Y, Faure M, Lin W, Wang QC and Ji WB. 2012a. Tectonics of the middle Triassic intracontinental Xuefengshan Belt, South China: New insights from structural and chronological constraints on the basal décollement zone. *International Journal of Earth Sciences*, 101 (8): 2125–2150
- Chu Y, Faure M, Lin W and Wang QC. 2012b. Early Mesozoic tectonics of the South China block: Insights from the Xuefengshan intracontinental orogen. *Journal of Asian Earth Sciences*, 61: 199–220
- Cui Y. 1989. Isotopic geochronology of Hetai granites and the genesis evolution. In: Conference Paper of the Fourth National Isotopic Meeting. 62–63 (in Chinese)
- Deng XG, Chen ZG, Li XH and Liu DY. 2004. SHRIMP U-Pb zircon dating of the Darongshan-Shiwandashan granitoid belt in southeastern Guangxi, China. *Geological Review*, 50 (4): 426–432 (in Chinese with English abstract)
- Ding RX, Zou HP, Lao MJ, Du XD, Zou YZ and Zeng CY. 2015. Indosinian activity records of ductile shear zones in southern segment of Qin-Hang combined belt: A case study of Fangcheng-Lingshan fault zone. *Earth Science Frontiers*, 22 (2): 79–85 (in Chinese with English abstract)
- England PC and Thompson A. 1986. Some thermal and tectonic models for crustal melting in continental collision zones. In: Coward MP and Ries AC (eds.). *Table of Contents*. Geological Society, London, Special Publication, 19: 83–94
- Feng SJ, Zhao KD, Ling HF, Chen PR, Chen WF, Sun T, Jiang SY and Pu W. 2014. Geochronology, elemental and Nd-Hf isotopic geochemistry of Devonian A-type granites in central Jiangxi, South China: Constraints on petrogenesis and post-collisional extension of the Wuyi-Yunkai Orogeny. *Lithos*, 206–207: 1–18
- Foster MD. 1960. Interpretation of the composition of trioctahedral micas. Washington: US Government Printing Office, 11–49
- Guo FX. 1994. Geotectonic units of Guangxi. *Journal of Guilin College of Geology*, 14(3): 233–243 (in Chinese with English abstract)
- Harris N, Ayres M and Massey J. 1995. Geochemistry of granitic melts produced during the incongruent melting of muscovite: Implications for the extraction of Himalayan leucogranite magmas. *Journal of Geophysical Research*, 100 (B8): 15767–15777
- Harris NBW and Inger S. 1992. Trace element modelling of pelite-derived granites. *Contributions to Mineralogy and Petrology*, 110(1): 46–56
- Healy B, Collins WJ and Richards SW. 2004. A hybrid origin for Lachlan S-type granites: The Murrumbidgee batholith example. *Lithos*, 79(1–2): 197–216
- Henry DJ, Guidotti CV and Thomson JA. 2005. The Ti-saturation surface for low-to-medium pressure metapelitic biotites: Implications for geothermometry and Ti-substitution mechanisms. *American Mineralogist*, 90(2–3): 316–328
- Huang JQ, Ren JS, Jiang CF, Zhang ZK and Qin DY. 1987. *Geotectonic Evolution of China*. Berlin: Springer, 1–203
- Jiao QQ, Deng T, Wang LX, Xu DR, Chi GX, Chen GW, Liu M, Chen YS, Gao YW and Zou SH. 2017. Geochronological and mineralogical constraints on mineralization of the Hetai goldfield in Guangdong Province, South China. *Ore Geology Reviews*, 88: 655–673
- Jiao QQ, Xu DR, Chen GW, Chen YS, Zhang JL, Gao YW, Yu LL and Zou SH. 2017. Zircon LA-ICP-MS U-Pb age of mylonite in the Hetai goldfield, Guangdong Province of South China and the geological implication. *Acta Petrologica Sinica*, 33 (6): 1755–1774 (in Chinese with English abstract)
- Jiao SJ, Li XH, Huang HQ and Deng XG. 2015. Metasedimentary melting in the formation of charnockite: Petrological and zircon U-Pb-Hf-O isotope evidence from the Darongshan S-type granitic complex in southern China. *Lithos*, 239: 217–233
- Johannes W, Ehlers C, Kriegsman LM and Mengel K. 2003. The link between migmatites and S-type granites in the Turku area, southern Finland. *Lithos*, 68(3–4): 69–90
- Jung S, Hoernes S and Mezger K. 2000. Geochronology and petrogenesis of Pan-African, syn-tectonic, S-type and post-tectonic A-type granite (Namibia): Products of melting of crustal sources, fractional crystallization and wall rock entrainment. *Lithos*, 50(4): 259–287
- Kang YJ. 2001. On the geological features of the Yunkai metamorphosed terrain. *Geoscience*, 15 (3): 275–280 (in Chinese with English abstract)
- Kuang YG, Huang YH, Zhuang WM, Zhuo WH and Xiao SM. 2001. Establishment of the Yunkai Group-complex in western Guangdong: A new understanding of pre-Devonian metamorphic strata in the Yunkai area. *Regional Geology of China*, 20(2): 146–152 (in Chinese with English abstract)
- Li SG, Xiao YL, Liou D, Chen YZ, Ge NJ, Zhang ZQ, Sun SS, Cong BL, Zhang RY, Hart SR and Wang SS. 1993. Collision of the North China and Yangtze blocks and formation of coesite-bearing eclogites: Timing and processes. *Chemical Geology*, 109 (1–4): 89–111
- Li XH, Li ZX, Wingate MTD, Chung SL, Liu Y, Lin GC and Li WX. 2006. Geochemistry of the 755Ma Mundine Well dyke swarm, northwestern Australia: Part of a Neoproterozoic mantle superplume beneath Rodinia? *Precambrian Research*, 146(1–2): 1–15
- Li ZX, Li XH, Wartho JA, Clark C, Li WX, Zhang CL and Bao CM. 2010. Magmatic and metamorphic events during the Early Paleozoic Wuyi-Yunkai Orogeny, southeastern South China: New age constraints and pressure-temperature conditions. *GSA Bulletin*, 122 (5–6): 772–793
- Liang XQ and Li XH. 2005. Late Permian to middle Triassic sedimentary records in Shiwandashan basin: Implication for the Indosinian Yunkai Orogenic Belt, South China. *Sedimentary Geology*, 177(3–4): 297–320
- Lin W, Wang QC and Chen K. 2008. Phanerozoic tectonics of South China Block: New insights from the polyphase deformation in the Yunkai Massif. *Tectonics*, 27(6): TC6004
- Lin WW and Peng LJ. 1994. The estimation of Fe³⁺ and Fe²⁺ contents in amphibole and biotite from EPMA data. *Journal of Changchun University of Earth Sciences*, 24 (2): 155–162 (in Chinese with English abstract)
- Liu HY, Montaser A, Dolan SP and Schwartz RS. 1996. Inter-laboratory note. Evaluation of a low sample consumption, high-efficiency nebulizer for elemental analysis of biological samples using inductively coupled plasma mass spectrometry. *Journal of Analytical Atomic Spectrometry*, 11(4): 307–311
- Liu YS, Hu ZC, Gao S, Günther D, Xu J, Gao CG and Chen HH. 2008. In situ analysis of major and trace elements of anhydrous minerals by LA-ICP-MS without applying an internal standard. *Chemical Geology*, 257(1–2): 34–43

- Liu YS, Hu ZC, Zong KQ, Gao CG, Gao S, Xu J and Chen HH. 2010. Reappraisal and refinement of zircon U-Pb isotope and trace element analyses by LA-ICP-MS. *Chinese Science Bulletin*, 55 (15): 1535–1546
- Ludwig KR. 2003. *Isoplot 3.00: A Geochronological Toolkit for Microsoft Excel*. Berkeley, CA: Berkeley Geochronology Center
- Mao JR, Takahashi Y, Kee WS, Li ZL, Ye HM, Zhao XL, Liu K and Zhou J. 2011. Characteristics and geodynamic evolution of Indosinian magmatism in South China: A case study of the Guikeng pluton. *Lithos*, 127(3–4): 535–551
- Middlemost EAK. 1994. Naming materials in the magma/igneous rock system. *Earth-Science Reviews*, 37(3–4): 215–224
- Milord I, Sawyer EW and Brown M. 2001. Formation of diatexite migmatite and granite magma during anatexis of semi-pelitic metasedimentary rocks: An example from St. Malo, France. *Journal of Petrology*, 42(3): 487–505
- Miyashiro A. 1978. Nature of alkalic volcanic rock series. *Contributions to Mineralogy and Petrology*, 66(1): 91–104
- Nachit H, Ibhi A, Abia EH and Ohoud MB. 2005. Discrimination between primary magmatic biotites, reequilibrated biotites and neofomed biotites. *Comptes Rendus Geoscience*, 337(6): 1415–1420
- Nam TN, Toriumi M and Itaya T. 1998. *P-T-t* paths and post-metamorphic exhumation of the Day Nui Con Voi shear zone in Vietnam. *Tectonophysics*, 290(3–4): 299–318
- Peng SB, Jin ZM, Liu YH, Fu JM, He LQ, Cai MH and Wang YB. 2006. Petrochemistry, chronology and tectonic setting of strong peraluminous Anatectic granitoids in Yunkai orogenic belt, western Guangdong Province, China. *Earth Science (Journal of China University of Geosciences)*, 31(1): 110–120 (in Chinese with English abstract)
- Qi CS, Deng XG, Li WX, Li XH, Yang YH and Xie LW. 2007. Origin of the Darongshan-Shiwandashan S-type granitoid belt from southeastern Guangxi: Geochemical and Sr-Nd-Hf isotopic constraints. *Acta Petrologica Sinica*, 23(2): 403–412 (in Chinese with English abstract)
- Qiu L, Yan DP, Zhou MF, Arndt NT, Tang SL and Qi L. 2014. Geochronology and geochemistry of the Late Triassic Longtan pluton in South China: Termination of the crustal melting and Indosinian orogenesis. *International Journal of Earth Sciences*, 103(3): 649–666
- Qiu XP. 2004. Relationship between gold mineralization and opening-closing cycle transition in the Yunkaidashan area, South China. *Geological Bulletin of China*, 23(3): 272–278 (in Chinese with English abstract)
- Qiu YX and Liang XQ. 2006. Evolution of basin-range coupling in the Yunkai Dashan-Shiwan Dashan area, Guangdong and Guangxi: With a discussion of several tectonic problems of south China. *Geological Bulletin of China*, 25(3): 340–347 (in Chinese with English abstract)
- Ren JS. 1991. On the geotectonics of southern China. *Acta Geologica Sinica*, 4(2): 111–130
- Ren JS. 1996. The continental tectonics of China. *Journal of Southeast Asian Earth Sciences*, 13(3–5): 197–204
- Roberts MP and Clemens JD. 1993. Origin of high-potassium, calc-alkaline, I-type granitoids. *Geology*, 21(9): 825–828
- Sawyer EW. 1994. Melt segregation in the continental crust. *Geology*, 22(11): 1019–1022
- Sawyer EW. 1998. Formation and evolution of granite magmas during crustal reworking: The significance of diatexites. *Journal of Petrology*, 39(6): 1147–1167
- Sawyer EW. 2001. Melt segregation in the continental crust: Distribution and movement of melt in anatectic rocks. *Journal of Metamorphic Geology*, 19(3): 291–309
- Sawyer EW. 2010. Migmatites formed by water-fluxed partial melting of a leucogranodiorite protolith: Microstructures in the residual rocks and source of the fluid. *Lithos*, 116(3–4): 273–286
- Sawyer EW, Cesare B and Brown M. 2011. When the continental crust melts. *Element*, 7(4): 229–234
- Sepahi AA, Borzoei K and Salami S. 2013. Mineral chemistry and thermobarometry of plutonic, metamorphic and anatectic rocks from the Tueyserkan area (Hamedan, Iran). *Geological Quarterly*, 57(3): 515–526
- Shabani AAT, Lalonde AE and Whalen JB. 2003. Composition of biotite from granitic rocks of the Canadian Appalachian orogen: A potential tectonomagmatic indicator? *The Canadian Mineralogist*, 41(6): 1381–1396
- Simpson RL, Parrish RR, Searle MP and Waters DJ. 2000. Two episodes of monazite crystallization during metamorphism and crustal melting in the Everest region of the Nepalese Himalaya. *Geology*, 28(5): 403–406
- Sláma J, Košler J, Condon DJ, Crowley JL, Gerdes A, Hanchar JM, Horstwood MSA, Morris GA, Nasdala L, Norberg N, Schaltegger U, Schoene B, Tubrett MN and Whitehouse MJ. 2008. Plešovice zircon: A new natural reference material for U-Pb and Hf isotopic microanalysis. *Chemical Geology*, 249(1–2): 1–35
- Solar GS and Brown M. 2001. Petrogenesis of migmatites in Maine, USA: Possible source of peraluminous leucogranite in plutons? *Journal of Petrology*, 42(4): 789–823
- Suga K, Yui TF, Shellnutt JG, Wu TW, Mori Y, Miyazaki K and Jahn BM. 2016. Nd-Sr isotopic constraint to the formation of metatexite and diatexite migmatites, Higo metamorphic terrane, central Kyushu, Japan. *International Geology Review*, 58(4): 405–423, doi: 10.1080/00206814.2015.1086961
- Sun SS and McDonough WF. 1989. Chemical and isotopic systematics of oceanic basalts: Implications for mantle composition and processes. In: Saunders AD and Norry MJ (eds.). *Magmatism in the Ocean Basins*. Geological Society, London, Special Publication, 42(1): 313–345
- Sun T, Zhou XM, Chen PR, Li HM, Zhou HY, Wang ZC and Shen WZ. 2005. Strongly peraluminous granites of Mesozoic in eastern Nanling range, southern China: Petrogenesis and implications for tectonics. *Science in China (Series D)*, 48(2): 165–174
- Sun T. 2006. A new map showing the distribution of granites in South China and its explanatory notes. *Geological bulletin of China*, 25(3): 332–335 (in Chinese with English abstract)
- Uchida E, Endo S and Makino M. 2007. Relationship between solidification depth of granitic rocks and formation of hydrothermal ore deposits. *Resource Geology*, 57(1): 47–56
- Wan TF. 2012. *The Tectonics of China: Data, Maps and Evolution*. Berlin: Springer
- Wan YS, Liu DY, Wilde SA, Cao JJ, Chen B, Dong CY, Song B and Du LL. 2010. Evolution of the Yunkai Terrane, South China: Evidence from SHRIMP zircon U-Pb dating, geochemistry and Nd isotope. *Journal of Asian Earth Sciences*, 37(2): 140–153
- Wang JC, Wang ZY, Geng WH, Yiin YQ and Yang MS. 1994. Discovery and significance of large detachment faults in the western margin of Yunkai Uplift. *Chinese Science Bulletin*, 40(16): 1369–1373
- Wang KZ, Yan TZ and Yuan Q. 2006. Characteristics of Caledonian folds in the northern segment of the Yangtze platform: Evidence from unconformity. *Geological Bulletin of China*, 25(6): 673–675 (in Chinese with English abstract)
- Wang LK, Sha LK, Xu WX, Deng GQ, Zhang SL and Liang YL. 2003. *The Theory of Granite Formation and Series*. Guangzhou: Guangdong Science and Technology Press (in Chinese)
- Wang YJ, Fan WM, Zhao GC, Ji SC and Peng TP. 2007a. Zircon U-Pb geochronology of gneissic rocks in the Yunkai massif and its implications on the Caledonian event in the South China Block. *Gondwana Research*, 12(4): 404–416
- Wang YJ, Fan WM, Cawood PA, Ji SC, Peng TP and Chen XY. 2007b. Indosinian high-strain deformation for the Yunkaidashan tectonic belt, South China: Kinematics and ⁴⁰Ar/³⁹Ar geochronological constraints. *Tectonics*, 26(6): TC6008
- Wang YJ, Zhang AM, Fan WM, Peng TP, Zhang FF, Zhang YZ and Bi XW. 2010. Petrogenesis of Late Triassic post-collisional basaltic

- rocks of the Lancangjiang tectonic zone, southwest China, and tectonic implications for the evolution of the eastern Paleotethys: Geochronological and geochemical constraints. *Lithos*, 120(3-4): 529-546
- Wang YJ, Zhang AM, Fan WM, Zhao GC, Zhang GW, Zhang YZ, Zhang FF and Li SZ. 2011. Kwangian crustal anatexis within the eastern South China Block: Geochemical, zircon U-Pb geochronological and Hf isotopic fingerprints from the gneissoid granites of Wugong and Wuyi-Yunkai domains. *Lithos*, 127(1-2): 239-260
- Wang YJ, Wu CM, Zhang AM, Fan WM, Zhang YH, Zhang YZ, Peng TP and Yin CQ. 2012. Kwangian and Indosinian reworking of the eastern South China Block: Constraints on zircon U-Pb geochronology and metamorphism of amphibolites and granulites. *Lithos*, 150: 227-242
- Wang YJ, Fan WM, Zhang GW and Zhang YH. 2013. Phanerozoic tectonics of the South China block: Key observations and controversies. *Gondwana Research*, 23(4): 1273-1305
- Ward R, Stevens G and Kisters A. 2008. Fluid and deformation induced partial melting and melt volumes in low-temperature granulite-facies metasediments, Damara Belt, Namibia. *Lithos*, 105(3-4): 253-271
- Whalen JB, Currie KL and Chappell BW. 1987. A-type granites: Geochemical characteristics, discrimination and petrogenesis. *Contributions to Mineralogy and Petrology*, 95(4): 407-419
- White RW, Pomroy NE and Powell R. 2005. An in situ metatexite-diatexite transition in upper amphibolite facies rocks from Broken Hill, Australia. *Journal of Metamorphic Geology*, 23(7): 579-602
- Yan DP, Zhou MF, Wang CY and Xia B. 2006. Structural and geochronological constraints on the tectonic evolution of the Dulong-Song Chay tectonic dome in Yunnan province, SW China. *Journal of Asian Earth Sciences*, 28(4-6): 332-353
- Ye BD. 1989. Isotopic ages of the Yunkai area, Guangdong and Guangxi provinces, and the geological implication. *Guangdong Geology*, 4(3): 39-55 (in Chinese with English abstract)
- Ye ZH, Lao QY and Hu SL. 2000. Some remarks on the geologic age and stratigraphic sequence of Yunkai Group in Yunkai Mountains. *Geological Review*, 46(5): 449-454 (in Chinese with English abstract)
- Yuan HL, Wu FY, Gao S, Liu XM, Xu P and Sun DY. 2003. LA-ICPMS zircon U-Pb age and the trace elements from Cenozoic pluton in Northeast China. *Chinese Science Bulletin*, 48(14): 1511-1520 (in Chinese)
- Yuan HL, Gao S, Liu XM, Li HM, Günther D and Wu FY. 2004. Accurate U-Pb age and trace element determinations of zircon by laser ablation-inductively coupled plasma-mass spectrometry. *Geostandards and Geoanalytical Research*, 28(3): 353-370
- Zhai W, Yuan GB, Li ZL, Huang DL and Wen YJ. 2005. U-Pb isotope age of zircons in gold-bearing quartz veins from the Hetai gold deposit, western Guangdong, China: Constraints on the timing of gold metallogenesis. *Geological Review*, 51(3): 340-346 (in Chinese with English abstract)
- Zhang BY and Yu HN. 1992. The genetic relationship of mylonites, migmatites and granites: With special reference to the deep-level nappe structure in western Guangdong. *Geological Review*, 38(5): 407-413 (in Chinese with English abstract)
- Zhao KD, Jiang SY, Chen WF, Chen PR and Ling HF. 2013. Zircon U-Pb chronology and elemental and Sr-Nd-Hf isotope geochemistry of two Triassic A-type granites in South China: Implication for petrogenesis and Indosinian transtensional tectonism. *Lithos*, 160-161: 292-306
- Zheng YF. 2008. A perspective view on ultrahigh-pressure metamorphism and continental collision in the Dabie-Sulu orogenic belt. *Chinese Science Bulletin*, 53(20): 3081-3104
- Zhou XM. 2007. *Petrogenesis of Late Mesozoic Granitoids in the Nanling Region and Dynamical Evolution of the Lithosphere*. Beijing: Science Press (in Chinese)
- Zhou XY, Yu JH, Wang LJ, Shen LW and Zhang CH. 2015. Compositions and formation of the basement metamorphic rocks in Yunkai terrane, western Guangdong Province, South China. *Acta Petrologica Sinica*, 31(5): 855-882 (in Chinese with English abstract)

附中文参考文献

- 蔡明海, 战明国, 彭松柏, 孟祥金, 刘国庆. 2002. 云开地区中生代成矿地质背景及成矿动力学机制研究. *矿床地质*, 21(3): 264-269
- 陈骏, 王鹤年. 1993. 广东省河台含金剪切带中 REE 及其它微量元素含量和分布特征. *矿床地质*, 12(3): 202-211
- 崔遥. 1989. 河台花岗岩同位素地质年代学及成因演化. 见: 第四届全国同位素会议论文(摘要)汇编. 62-63
- 邓希光, 陈志刚, 李献华, 刘敦一. 2004. 桂东南地区大容山-十万大山花岗岩带 SHRIMP 锆石 U-Pb 定年. *地质论评*, 50(4): 426-432
- 丁汝鑫, 邹和平, 劳妙姬, 杜晓东, 周永章, 曾长育. 2015. 钦-杭结合带南段韧性剪切带印支期活动记录: 以防城-灵山断裂带为例. *地学前缘*, 22(2): 79-85
- 广西壮族自治区地质矿产局. 1985. 广西壮族自治区区域地质志. 北京: 地质出版社
- 郭福祥. 1994. 广西大地构造单元. *桂林冶金地质学院学报*, 14(3): 233-243
- 湖南省地质矿产局. 1988. 湖南省区域地质志. 北京: 地质出版社
- 焦骞骞, 许德如, 陈根文, 陈延生, 张建岭, 高亦文, 于亮亮, 邹少浩. 2017. 广东省河台金矿区糜棱岩锆石 LA-ICP-MS U-Pb 年龄及其地质意义. *岩石学报*, 33(6): 1755-1774
- 康云骥. 2001. 云开变质地体的地质特征. *现代地质*, 15(3): 275-280
- 邝永光, 黄宇辉, 庄文明, 卓伟华, 肖思明. 2001. 粤西云开岩群的建立——云开地区前泥盆纪变质地层的再认识. *地质通报*, 20(2): 146-152
- 林文蔚, 彭丽君. 1994. 由电子探针分析数据估算角闪石、黑云母中的 Fe^{3+} 、 Fe^{2+} . *长春地质学院学报*, 24(2): 155-162
- 彭松柏, 金振民, 刘云华, 付建明, 何龙清, 蔡明海, 王彦斌. 2006. 云开造山带强过铝深熔花岗岩地球化学、年代学及构造背景. *地球科学(中国地质大学学报)*, 31(1): 110-120
- 祁昌实, 邓希光, 李武显, 李献华, 杨岳衡, 谢烈文. 2007. 桂东南大容山-十万大山 S 型花岗岩带的成因: 地球化学及 Sr-Nd-Hf 同位素制约. *岩石学报*, 23(2): 403-412
- 邱小平. 2004. 两广云开大山地区开合旋回转换与金成矿作用的关系. *地质通报*, 23(2): 272-278
- 丘元禧, 梁新权. 2006. 两广云开大山-十万大山地区盆山耦合构造演化——兼论华南若干区域构造问题. *地质通报*, 25(3): 340-347
- 孙涛. 2006. 新编华南花岗岩分布图及其说明. *地质通报*, 25(3): 332-335
- 汪劲草, 王正云, 耿文辉, 尹意求, 杨明寿. 1994. 云开隆起西缘大型剥离断层的发现及意义. *科学通报*, 39(20): 1886-1888
- 王孔忠, 颜铁增, 袁强. 2006. 扬子东南缘北段加里东期的褶皱特征——来自不整合深部的证据. *地质通报*, 25(6): 673-675
- 王联魁, 沙连堃, 徐文新, 邓高强, 张绍立, 梁跃龙. 2003. 论花岗

- 岩建造与系列——兼论花岗岩三级成因分类. 广州: 广东科技出版社
- 叶伯丹. 1989. 两广云开地区同位素地质年龄数据及其地质意义. 广东地质, 4(3): 39-55
- 叶真华, 劳秋元, 胡世玲. 2000. 云开大山云开群地层时代和层序的研究现状与新认识. 地质论评, 46(5): 449-454
- 袁洪林, 吴福元, 高山, 柳小明, 徐平, 孙德有. 2003. 东北地区新生代侵入体的锆石激光探针 U-Pb 年龄测定与稀土元素成分分析. 科学通报, 48(14): 1511-1520
- 翟伟, 袁桂邦, 李兆麟, 黄栋林, 文拥军. 2005. 粤西河台金矿床富硫化物含金石英脉锆石 U-Pb 测年及成矿意义. 地质论评, 51(3): 340-346
- 张伯有, 俞鸿年. 1992. 糜棱岩、混合岩、花岗岩三者成因联系——粤西深层次推覆构造研究的特殊意义. 地质论评, 38(5): 407-413
- 周新民. 2007. 南岭地区晚中生代花岗岩成因与岩石圈动力学演化. 北京: 科学出版社
- 周雪瑶, 于津海, 王丽娟, 沈林伟, 张春晖. 2015. 粤西云开地区基底变质岩的组成和形成. 岩石学报, 31(3): 855-882